Biomedicine & Pharmacotherapy 192 (2025) 118652

Contents lists available at ScienceDirect

Biomedicine & Pharmacotherapy

journal homepage: www.elsevier.com/locate/biopha

Phosphatidylcholine-bound palmitoleic acid: A bioactive key to unlocking macrophage anti-inflammatory functions

Miguel A. Bermúdez [a,c,d,1], Clara Meana [b,c,e,1], Alvaro Garrido [a,c], Alfonso Pérez-Encabo [f], María A. Balboa [b,c], Jesús Balsinde [a,c,*]

[a] Bioactive Lipids and Lipidomics Core, IBGM, CSIC-UVA, Valladolid 47003, Spain
[b] Lipid Metabolism and Inflammation Group, IBGM, CSIC-UVA, Valladolid 47003, Spain
[c] Centro de Investigación Biomédica en Red de Diabetes y Enfermedades Metabólicas Asociadas (CIBERDEM), Instituto de Salud Carlos III, 28029, Madrid, Spain
[d] Facultad de Ciencias y Artes, Universidad Católica de Ávila (UCAV), Ávila 05005, Spain
[e] Departamento de Pediatría e Inmunología, Universidad de Valladolid, Valladolid 47005, Spain
[f] Instituto CINQUIMA, Departamento de Química Orgánica, Universidad de Valladolid, Valladolid 47011, Spain

ARTICLE INFO

Keywords:
Palmitoleic acid
Lipid signaling
Macrophage activation
Lipid-mediated immunomodulation
NF-κB signaling
Inflammation

ABSTRACT

Inflammatory processes are central to the progression of numerous chronic conditions, including cardiovascular and metabolic disorders, with macrophages playing a pivotal role in these responses. Monounsaturated fatty acids, including palmitoleic acid (16:1 n − 7), have been implicated in modulating inflammation, yet their precise molecular mechanisms of action remain incompletely understood. Notably, in macrophages, 16:1 n − 7 is preferentially esterified into a specific phosphatidylcholine (PC) species, PC(16:0/16:1 n − 7), raising the possibility that its biological activity is governed by this lipid-bound form. Here, we demonstrate that the anti-inflammatory effects of 16:1 n − 7 in macrophages are mediated through its incorporation into this PC species. Using synthetic phospholipids and multiple activation stimuli, we show that PC(16:0/16:1 n − 7) directly regulates macrophage activation. It suppresses NF-κB signaling, reprograms gene expression, and promotes a shift toward an anti-inflammatory, M2-like phenotype that enhances phagocytic capacity. These effects are preserved in ether analogs resistant to phospholipase-mediated hydrolysis, confirming that the release of free 16:1 n − 7 is not required. These findings reveal a previously unrecognized lipid-driven mechanism of immunomodulation, in which specific structural features of PC(16:0/16:1 n − 7) confer intrinsic bioactivity. Our study broadens understanding of immunometabolic regulation by membrane phospholipids, and provides a mechanistic basis for the pharmacotherapeutic potential of defined lipid species in reprogramming macrophage function in inflammatory diseases.

1. Introduction

Monounsaturated fatty acids are widely acknowledged for their positive impact on human health, particularly in supporting cardiovascular health by reducing inflammation. Their unique physical characteristics, remaining in a liquid state at body temperature while resisting oxidation, make them valuable components of cell membranes. These properties are thought to help membranes maintain an ideal balance of fluidity, contributing to overall cellular stability and function [1,2]. Recent studies in murine models of metabolic disease have highlighted the potential anti-inflammatory role of palmitoleic acid (*cis*-9-hexadecenoic acid, 16:1 n − 7), a relatively minor monounsaturated fatty acid. Findings suggest that this fatty acid helps mitigate metabolic disorders by reducing hepatic steatosis and enhancing whole-body insulin sensitivity. Moreover, elevated circulating levels of 16:1 n − 7 appear to improve insulin responsiveness in muscle cells, support pancreatic β-cell function and proliferation, and protect against palmitate-induced stress and apoptosis across various cell types [3–10]. However, conflicting evidence also exists, particularly in humans. Some investigations have linked increased circulating levels of palmitoleic acid to adverse health outcomes, including obesity, pancreatitis, inflammatory bowel disease, hepatic steatosis, and cardiovascular

* Corresponding author at: Bioactive Lipids and Lipidomics Core, IBGM, CSIC-UVA, Valladolid 47003, Spain.
E-mail address: jbalsinde@uva.es (J. Balsinde).
[1] These authors contributed equally and are listed in alphabetical order

https://doi.org/10.1016/j.biopha.2025.118652
Received 17 July 2025; Received in revised form 2 October 2025; Accepted 16 October 2025

conditions [10–15]. Thus, the behavior of 16:1 n − 7 in physiology and pathophysiology is intriguing, and its effects appear to be highly compartmentalized. It has been suggested that the marked tissue-specific formation of 16:1 n − 7 may underlie much of the discordance observed [16–19].

Despite the growing biomedical interest in its significance, the precise mechanisms through which 16:1 n − 7 influences cellular signaling and molecular pathways remain largely unknown [20]. In the current study, we aim to fill these gaps by providing novel and unexpected insights into the molecular mechanisms triggered by 16:1 n − 7 in major immunoinflammatory cells such as macrophages. Given the alarming prevalence of inflammatory metabolic disorders like diabetes and cardiovascular disease, advancing our molecular understanding of 16:1 n − 7 effects could be instrumental in developing effective treatments. This progress would not only improve public health by enhancing life expectancy and well-being but also yield significant economic benefits, considering the high costs associated with treating these widespread conditions.

In previous work, we performed comprehensive analyses of the incorporation, distribution, and utilization of 16:1 n − 7 in key immunoinflammatory cells, including human monocytes and murine macrophages [21–24]. These studies revealed striking features in how the cells process 16:1 n − 7. Most of the fatty acid is concentrated within the phosphatidylcholine (PC) fraction, with a notable dominance of a unique species: 1-palmitoyl-2-palmitoleoyl-*sn*-glycero-3-phosphocholine, PC(16:0/16:1 n − 7) [22,23]. Interestingly, upon activation by innate immune stimuli, monocytes and macrophages rapidly shuttle 16:1 n − 7 moieties from PC to phosphatidylinositol (PI), a process requiring the formation of free 16:1 n − 7 as an intermediate [24]. Whether this phospholipid remodeling pathway contributes to the biological activity of 16:1 n − 7 remains unknown. In this regard, there is a tendency to assume that the biologically active form of 16:1 n − 7 is its free fatty acid form, though this has never been conclusively proven. Given the unique distribution of 16:1 n − 7 in innate immune cells, we sought to investigate the effects of introducing PC(16:0/16:1 n − 7) to the cells and examining its metabolism, rather than simply adding free 16:1 n − 7, as is commonly done in most studies exploring the biological effects of the fatty acid. Our findings demonstrate that it is the complete 16:1 n − 7-containing phospholipid, rather than the free fatty acid form, that is responsible for the pronounced anti-inflammatory activity characteristic of 16:1 n − 7. Furthermore, macrophages loaded with 16:1 n − 7-containing PC undergo gene expression reprogramming, likely driven by the restrained activity of the NF-κB transcription factor. This process leads to the acquisition of an anti-inflammatory phenotype and, consequently, an enhanced phagocytic capacity. Our findings suggest that 16:1 n − 7-containing PC plays a role in regulating macrophage polarization and shaping their inflammatory behavior. Given that macrophages can repolarize under appropriate cytokine conditions, the presence of 16:1 n − 7-containing PC in the membrane may help sustain a polarized M2-like anti-inflammatory state.

2. Materials and methods

2.1. Cell culture

Resident peritoneal macrophages from Swiss male mice (University of Valladolid Animal House, 10–12 weeks old) were obtained by peritoneal lavage using 5 ml cold phosphate-buffered saline, as described elsewhere [25]. The cells were plated at 2×10^6 per well (6-well plates) in 2 ml RPMI 1640 medium with 10 % fetal bovine serum, 100 U/ml penicillin, and 100 μg/ml streptomycin, and allowed to adhere for 20 h in a humidified atmosphere of 5 % CO_2 at 37 °C. All procedures involving animals were carried out under the supervision of the Institutional Committee of Animal Care and Usage of the University of Valladolid, and are in accordance with the guidelines established by the Spanish Ministry of Agriculture, Food, and Environment and the European Union.

For experiments, the cells were treated with the different phospholipids for the indicated periods of time. The phospholipids were added to cells as complexes with fatty acid free-bovine serum albumin (3:1). The complexes were formed by sonication in a water bath [26]. Afterward, the cells were placed in serum-free medium for 1 h before addition of stimulants for the indicated concentrations and periods of time. Zymosan was prepared as described [27]. For opsonization, the particles were treated with mouse serum (3 mg zymosan per 1 ml serum) for 20 min at 37 °C. Only zymosan preparations that showed no endogenous phospholipase A_2 activity, as measured by enzyme assay [28–30], were used in this study. Protein was measured according to Bradford [31], using a commercial kit (BioRad, Hercules, CA, USA).

For the antisense inhibition experiments, RAW264.7 macrophage-like cells were used. These cells were grown in DMEM supplemented with 10 % (v/v) fetal bovine serum, 100 U/ml penicillin, 100 μg/ml streptomycin, and 2 mM L-glutamine at 37 °C in a humidified atmosphere of 5 % CO_2 at 37 °C, as previously described [32,33]. The iPLA$_2$β antisense oligonucleotide utilized in this work has been described in previous studies [23,27]. The oligonucleotides were mixed with Lipofectamine RNAiMAX (Thermo Fisher Scientific, Walthman, MA, USA), following the manufacturer's instructions. Oligonucleotide treatment and culture conditions were not toxic for the cells as assessed by the trypan blue dye exclusion assay.

2.2. Lipid analysis by mass spectrometry

Total lipids from approximately 10^7 cells were extracted according to Bligh and Dyer [34]. After addition of internal standards, phospholipids were separated from neutral lipids by thin-layer chromatography, using *n*-hexane/diethyl ether/acetic acid (70:30:1, v/v/v) [35]. Phospholipid classes were separated with chloroform/methanol/28 % (w/w) ammonium hydroxide (60:37.5:4, v/v/v) as the mobile phase, using plates impregnated with boric acid [36]. Fatty acid methyl esters were obtained from the various lipid fractions by transmethylation with 0.5 M KOH in methanol for 60 min at 37 °C [21,22]. Analysis was carried out using an Agilent 7890A gas chromatograph coupled to an Agilent 5975C mass-selective detector operated in electron impact mode, equipped with an Agilent 7693 autosampler and an Agilent DB23 column (60 m length x 0.25 mm internal diameter x 0.15 μm film thickness). Data analysis was carried out with the Agilent G1701EA MSD Productivity Chemstation software, revision E.02.00 (Agilent Technologies, Santa Clara, CA, USA).

2.3. Real-time PCR

Total RNA was extracted using Trizol reagent (Ambion, Thermo Fisher Scientific). The cDNA templates were synthesized using Verso cDNA synthesis kit (Thermo Fisher Scientific), following the manufacturer's instructions. Quantitative PCR (qPCR) was carried out with an ABI 7500 machine (Applied Biosystems, Carlsbad, CA) using Brilliant III Ultra-Fast SYBR Green qPCR Master Mix (Agilent Technologies, Santa Clara, CA), and specific primers for each gene of interest. Primers used were: *Actb,* GGCTGTATTCCCCTCCATCG and CCAGTTGGTAACAATGCCATGT; *Fizz* (*Retnla*), CCAATCCAGCTAACTATCCCTCC *and* ACCCAGTAGCAGTCATCCCA; *Il10*, GCTCTTACTGACTGGCATGAG and CGCAGCTCTAGGAGCATGTG; *Il1b*, GCAACTGTTCCTGAACTCAACT and TCTTTTGGGGTCCGTCAACT; *Il6*, TAGTCCTTCCTACCCCAATTTCC and TTGGTCCTTAGCCACTCCTTC; *Nlrp3*, ATCAACAGGCGAGACCTCTG and GTCCTCCTGGCATACCATAG; *Ppib* (cyclophilin B), GGCTCCGTCGTCTTCCTTTT and ACTCGTCCTACAGATTCATCTCC; *Tnf*, ACGGCATGGATCTCAAAGAC and AGATAGCAAATCGGCTGACG; *Ym1* (*Chil3*), CAGGTCTGGCAATTCTTCTGAA and GTCTTGCTCATGTGTGTAAGTGA. The relative mRNA abundance for a given gene was calculated using the algorithm $2^{-\Delta\Delta Ct}$, with *Actb* and *Ppib* as internal standards [37].

2.4. Cytokine assays

Supernatants from cell cultures were obtained and cleared by centrifugation at 15,000 × *g* for 10 min. A volume of 100 µl was subsequently used for the assays. Quantification of TNF-α (catalog #88–7324–88), IL-6 (catalog #88–7064–88), and IL-1β (catalog no. 88–7013A-88) was carried out using commercial specific ELISA kits, following the indications of the manufacturer (Invitrogen, Thermo Fisher Scientific).

2.5. Immunofluorescence

Immunofluorescence staining was performed to assess NF-κB p65 nuclear translocation. Briefly, macrophages were seeded in glass coverslips at 1.5×10^5 cells/well in 12-well plates and incubated overnight. Cells were treated or left untreated with 100 µM PC(16:0/16:1 n − 7) or PC(16:0/16:116:1 n − 9) for 24 h, then exposed or not to 200 ng/ml LPS for the indicated times. After washing with PBS, cells were fixed with 4 % paraformaldehyde for 15 min, permeabilized with 0.3 % Triton X-100 for 3 min, and blocked with 10 % goat serum for 1 h. Afterward, the cells were incubated overnight at 4 °C with a rabbit NF-κB p65 antibody (1:200) (Cell Signaling, Danvers, MA, USA; catalog no. 8242) in 1 % goat serum, followed by a polyclonal anti-rabbit secondary antibody (Fab Alexa Fluor 594, 1:2000) (Life Technologies, Thermo Fisher Scientific; catalog no. A11072) for 1 h. DAPI staining (1 µg/ml) was performed for 5 min before mounting. A Leica TCS SP5X confocal microscope was used to visualize NF-κB and DAPI localization, and the translocation index was quantified using CellProfiler software. Three images per condition, containing 80–100 cells at similar confluence, were analyzed.

2.6. RNA-Seq analysis

Extracted RNA was sequenced at the Beijing Genomics Institute (BGI, Hong Kong, China) and data were analyzed by EGO Genomics (Salamanca, Spain). RNA-Seq quality control was performed with FastQC (v0.11.9) for each FASTQ file, and results were aggregated using MultiQC (https://www.bioinformatics.babraham.ac.uk/projects/fastqc/). Reads were aligned to the reference genome (GRCm39) with STAR, version 2.7.6 [38], and gene counts were estimated using featureCounts, version 2.0.1 [39]. Differential expression analysis was carried out in R, version 4.1.2. Count values were processed with edgeR, version 3.36.0 [40], normalized using the trimmed mean of M values method, and lowly expressed genes (<1 count per million) were filtered out. Differentially expressed genes were identified using linear models implemented in Limma-Voom, version 3.50.3 [41]. Heatmaps were generated with heatmap3, version 1.1.9 [42]. A list of M2 genes compiled by Jablonski et al. [43] was analyzed, and Z-score–normalized logCPM values were visualized as a heatmap with a color code with white for lower expression and red for higher expression.

2.7. Cell fractionation

After the various treatments, cells were washed with ice-cold PBS and scraped into hypotonic lysis buffer (10 mM Tris-HCl, pH 7.5, 10 mM NaCl, 3 mM $MgCl_2$, 1.1 mM EGTA, supplemented immediately before use with 0.5 mM DTT and protease inhibitor cocktail) (catalog no. P-8340, Sigma). Samples were incubated on ice for 15 min. NP-40 was then added to a final concentration of 0.05 % (v/v), followed by vigorous mixing for 10 s to disrupt the plasma membrane. Homogenates were centrifuged at 800 × *g* for 2 min at 4 °C. The supernatants, corresponding to the cytoplasmic fraction, were collected and stored at −20 °C until use. Pellets were washed twice with the same hypotonic buffer, resuspended in hypertonic lysis buffer (20 mM HEPES, pH 7.4, 420 mM NaCl, 1.5 mM $MgCl_2$, 0.1 mM EGTA, 25 % (v/v) glycerol, supplemented immediately before use with 0.5 mM DTT and protease inhibitor cocktail), mixed vigorously for 10 s, and incubated for 30 min at 4 °C under constant agitation. Finally, samples were centrifuged at 12000 × g for 10 min at 4 °C, and the resulting supernatants, corresponding to the nuclear fraction, were collected and stored at −80 °C until use.

2.8. Western blotting

Cell homogenates were prepared by lysis in buffer containing 20 mM Tris-HCl pH 7.4, 150 mM NaCl, 1 mM EDTA, 1 mM EGTA, 5 mM $Na_4P_2O_7$, 50 mM β-glycerophosphate, 270 mM sucrose, 0.1 % 2-mercaptoethanol, 1 % Triton X-100, 100 µM PMSF, 1 mM Na_3VO_4, 10 mM NaF and a protease inhibitor cocktail. After centrifugation at 15000 g for 10 min, 50–100 µg of cellular protein was separated by SDS–PAGE and transferred to PVDF membranes. Membranes were blocked with 5 % non-fat dry milk or 5 % bovine serum albumin in PBS, and incubated with primary antibodies (1:1000) in PBS with 0.5 % non-fat dry milk and 0.1 % Tween 20. Antibodies against NF-κB p65 (catalog no 8242), and IκBα (catalog no 4814) were from Cell Signaling Technology (Danvers, MA, USA). Anti-β-actin (catalog no. A5441) was from Sigma, and anti-p84 nuclear matrix protein (catalog no ab487) was from Abcam (Cambridge, UK). HRP-conjugated secondary antibodies were used at 1:5000 dilution. Antibodies anti-rabbit IgG (catalog no NA9340) were from Amersham Biosciences (Chalfont St. Giles, UK) and anti-mouse IgG (catalog no 1706516) were from BioRad. Bands were visualized using an ECL chemiluminescent substrate (Amersham).

2.9. Flow cytometry

After cell collection, non-specific binding was blocked with 5 µg/ml anti-CD16/32 (clone 93, catalog no. 101301, BioLegend, San Diego, CA, USA) for 20 min at 4 °C. Cells were subsequently stained with 0.5 µg/ml anti-CD206 (clone C068C2, catalog no.141710, BioLegend). Fluorescence was acquired using a Cytek Aurora spectral flow cytometer (Cytek Biosciences, Fremont, CA, USA), and data were analyzed with FlowJo™ software (version 11, FlowJo LLC, Ashland, OR, USA). A minimum of 10000 cells was analyzed per sample.

2.10. Phagocytosis assay

Yeast-derived zymosan conjugated with Alexa Fluor 488 served as the phagocytic stimulus. Cells were plated onto glass coverslips, permitted to adhere, and exposed to the relevant phospholipids for 24 h. Zymosan, at a ratio of 10 particles per cell (approximately 0.2 mg per 10^6 cells), was added, followed by a 30-min incubation at 37 °C. Coverslips were then rinsed with PBS, relocated to plates maintained at 37 °C, and phagocytosis was allowed to proceed for an additional 30-min period. To stop the reaction, cells were fixed with 4 % paraformaldehyde in PBS containing 3 % sucrose for 15 min. Subsequently, paraformaldehyde was eliminated through three PBS washes. DAPI staining was performed by incubating cells with a 1 µg/ml solution of the dye in PBS for 10 min. Coverslips were mounted onto microscopy slides using 10 µl of polyvinyl alcohol solution, until fluorescence microscopy analysis. Imaging was conducted with a Leica TCS SP5X confocal microscope equipped with a white laser (470–670 nm) (Leica Microsystem, Wetzlar, Germany). Captured images were processed utilizing LAS AF version 2.6.3 (Leica) and ImageJ (https://imagej.net/ij/). The phagocytic index was determined by dividing the phagosome count by the total cell number per field, then multiplying the result by the percentage of phagocytosing cells, as previously reported [44–46].

2.11. Statistical analysis

Statistical analyses were performed using SigmaPlot software, version 14.0 (Systat Software Inc., San Jose, CA, USA). Data are presented as means ± SD, as indicated in the figure legends. Pairwise comparisons were performed using Student's *t*-test, while analyses involving three or more groups were conducted using one-way or two-

way ANOVA followed by the Holm–Sidak post hoc multiple comparison test. A p-value < 0.05 was considered statistically significant. Details of the statistical tests and sample sizes are provided in the figure legends.

3. Results

3.1. Lipidomic analysis of the incorporation of palmitoleoyl-containing phosphatidylcholine into macrophage lipids

Previous work from our laboratory showed that enriching macrophages with 16:1 n − 7 significantly reduces their responses to bacterial lipopolysaccharide (LPS), highlighting the anti-inflammatory properties of this fatty acid [21,22]. Given the strong tendency of 16:1 n − 7 to accumulate predominantly in a single phospholipid species, namely PC (16:0/16:1 n − 7) [22–24], we began this study by investigating whether treating the cells with the entire phospholipid, rather than the free fatty acid itself, would lead to similar outcomes. This is a key question with regard to the mode of delivery of a lipid active principle into a biological system, because phospholipids are generally less toxic than free fatty acids, allowing their use at higher concentrations, which in turn enhances potency and efficacy. For these experiments, a multigram synthesis procedure of PC(16:0/16:1 n − 7) was developed, the details of which are presented as supplemental material (Appendix A). The synthetic route devised enables the incorporation of enantiomerically pure fatty acids (*cis* > 95 %) into the *sn*-2 position of any PC molecule. The chemical structures of all phospholipid species synthesized for this study are shown in Fig. 1.

Fig. 2 illustrates the lipidomic changes observed in murine macrophages following exposure to PC(16:0/16:1 n − 7). With regard to their fatty acid composition, the PC(16:0/16:1 n − 7)-treated cells exhibited the expected elevated levels of both 16:0 and 16:1 n − 7 fatty acids. No significant decreases were observed in any other fatty acid, indicating that the cells accommodated the supply of exogenous phospholipid well (Fig. 2**A**). The vast majority of the added PC(16:0/16:1 n − 7) remained associated with PC, although very small increases in 16:1 n − 7 within PE were also detected (Fig. 2**B**). While statistically significant, these PE

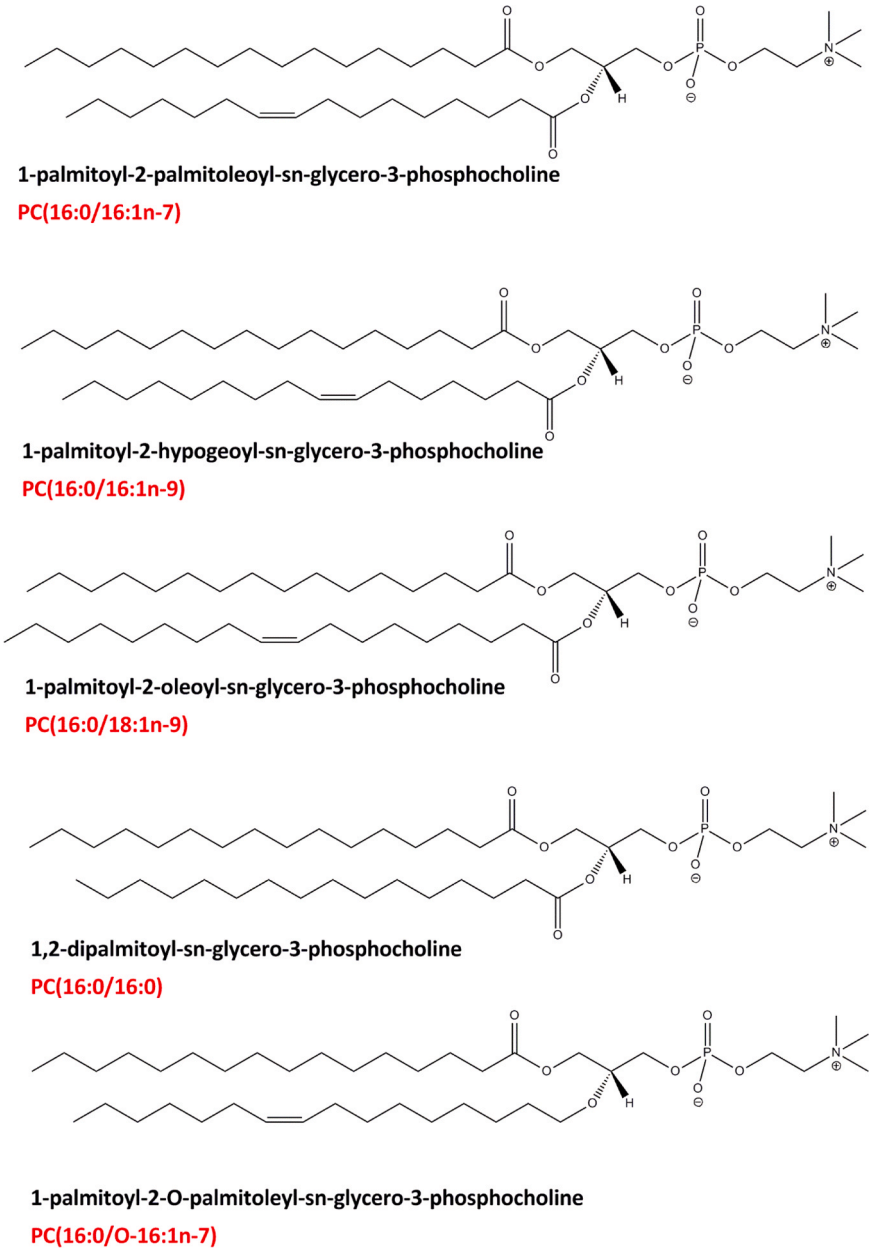

Fig. 1. Chemical structures of the phospholipid species synthesized for use in this study.

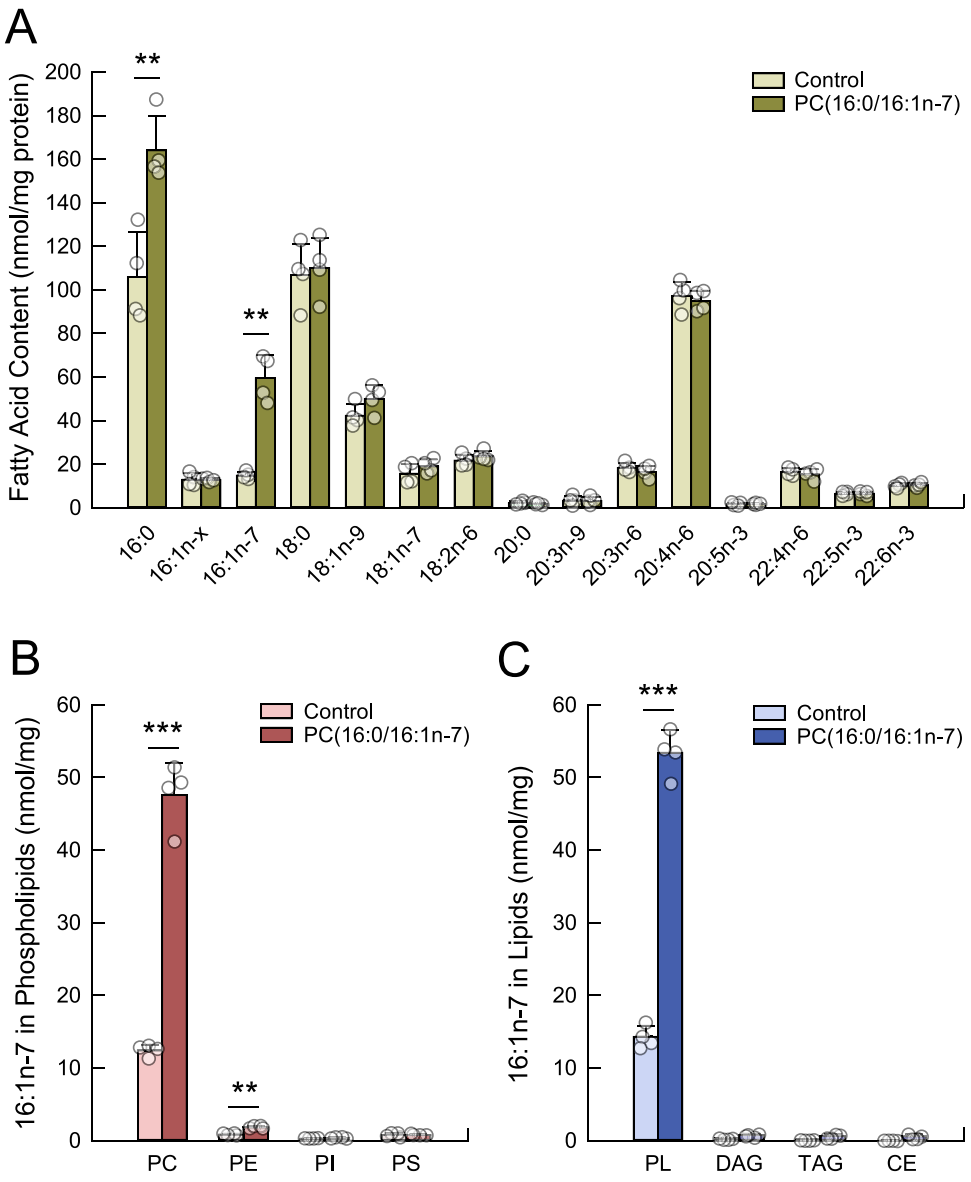

Fig. 2. Incorporation of PC(16:0/16:1 n − 7) into macrophages. The cells were treated with PC(16:0/16:1 n − 7) (100 μM, complexed with fatty acid free-bovine serum albumin at a 3:1 ratio) for 24 h. Total cellular fatty acids were determined by GC-MS (**A**). The 16:1 n − 7 content in phosphatidylcholine (PC), phosphatidylethanolamine (PE), phosphatidylinositol (PI), and phosphatidylserine (PS) was determined by GC-MS. 16:1 n − x denotes a mix of the n − 9 and n − 10 isomers, which elute together. (**B**) The 16:1n–7 content in phospholipids (PL), diacylglycerol (DAG), triacylglycerol (TAG), and cholesterol esters (CE) was determined by GC-MS (**C**). Results are shown as means ± SD of four independent determinations. ** $p < 0.01$, and *** $p < 0.001$, significantly different from the corresponding lipid in control cells using Student's *t*-test.

levels were so low compared to PC that they may simply reflect an inconsequential pathway of 16:1 n − 7 redistribution. No variations in the levels of 16:1 n − 7 were observed in any other phospholipid class (Fig. 2**B**) or in neutral lipids (Fig. 2**C**).

3.2. 16:1-containing PC species inhibit the expression of pro-inflammatory genes by activated macrophages

When PC(16:0/16:1 n − 7)-loaded macrophages were exposed to bacterial lipopolysaccharide (LPS), a markedly reduced expression of the pro-inflammatory genes *Il6*, *Tnf*, and of their respective protein products was observed (Fig. 3**A-D**). To demonstrate that this effect is specifically attributable to the presence of the 16:1 n − 7 moiety within the phospholipid, parallel experiments were also carried out with cells treated with other PC molecular species, where 16:1 n − 7 had been replaced with either oleic acid (18:1 n − 9, shown in the figure as PC (16:0/18:1 n − 9)), or palmitic acid (PC(16:0/16:0). Neither of these exerted a significant effect on the LPS-induced gene expression (Fig. 3**A** and **B**). As a positive control for these experiments, we also used PC (16:0/16:1 n − 9), that is, a species in which 16:1 n − 7 was replaced with its positional isomer hypogeic acid (16:1 n − 9), a fatty acid also known to exhibit a marked anti-inflammatory character [20–23]. Accordingly, PC(16:0/16:1-9) also strongly inhibited the LPS-induced upregulation of *Il6*, and *Tnf* (Fig. 3**A** and **B**). Overall, these findings provide detailed information to identify the minimal structural requirements necessary for the phospholipid to antagonize the LPS-induced gene expression responses. Thus, the effect appears to depend on the combined presence of a double bond within the fatty acid and a 16-carbon chain length, as 16:1 n − 7- and 16:1 n − 9-containing PCs are active, whereas 16:0- and 18:1 n − 9-containing PCs are not.

To further characterize the effect of PC(16:0/16:1 n − 7) on LPS-induced pro-inflammatory gene expression, concentration- and time-

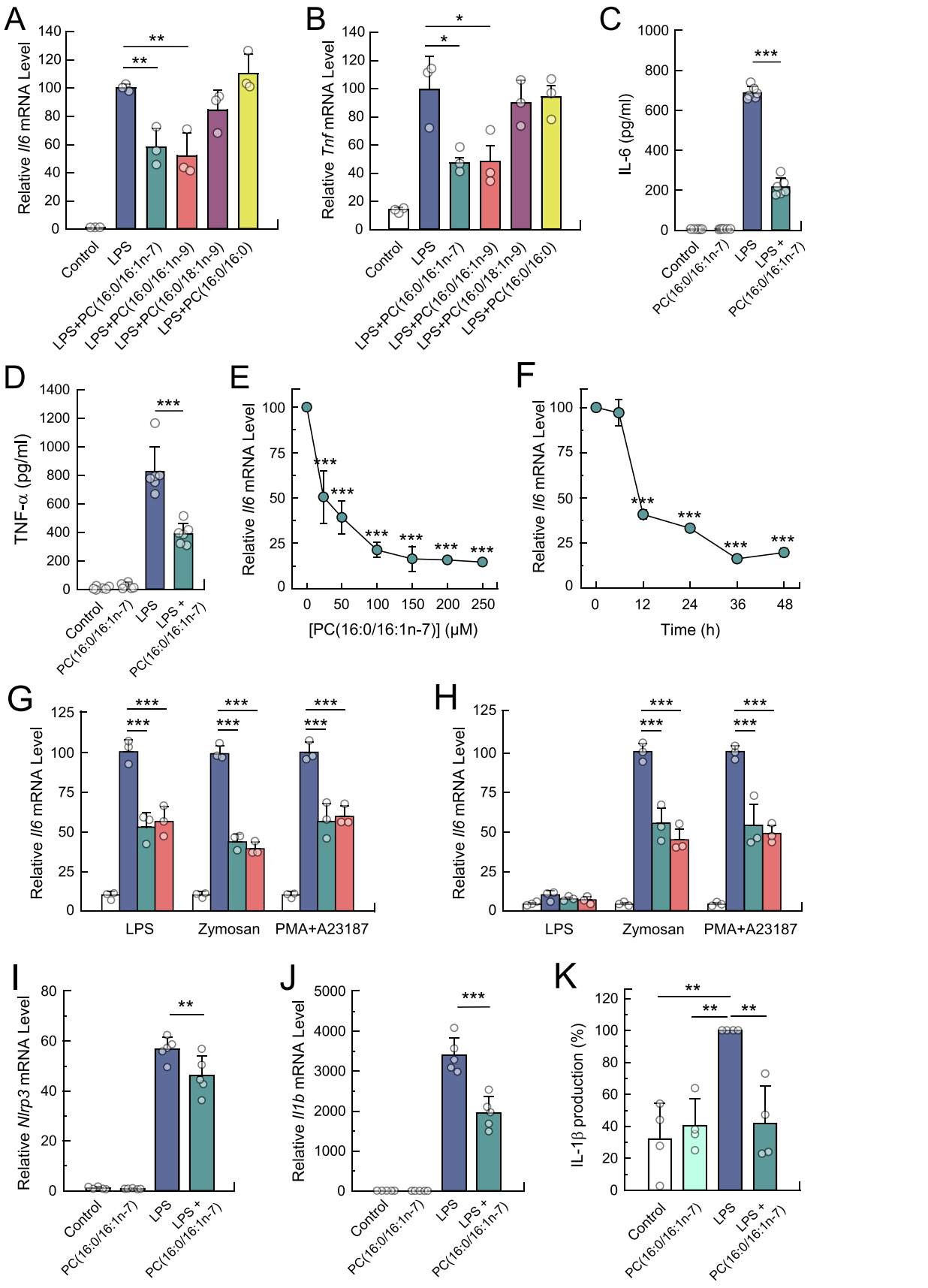

(caption on next page)

Fig. 3. Anti-inflammatory activity of PC(16:0/16:1 n − 7). (**A-D**) The cells were incubated with the indicated phospholipid (100 μM) for 24 h. Afterward, they were stimulated with 200 ng/ml LPS for 6 h. The mRNA expression levels for *Il6* (**A**), and *Tnf* (**B**), were analyzed by RT-qPCR. These data are given as means ± SD, n = 3; * $p < 0.05$, and ** $p < 0.01$, significantly different from the corresponding LPS stimulations in the absence of added phospholipid, by one-way ANOVA followed by the Holm-Sidak test. IL-6 (**C**) and TNF-α (**D**) levels in cell culture supernatants were analyzed using specific ELISAs. These data are given as means ± SD, n = 6; *** $p < 0.001$, significantly different from the corresponding LPS stimulations in the absence of added phospholipid, by one-way ANOVA followed by the Holm-Sidak test. (**E**) Concentration dependence of the effect of PC(16:0/16:1 n − 7). The cells were incubated with the indicated concentrations PC(16:0/16:1 n − 7) for 24 h and, afterward, stimulated with 200 ng/ml LPS for 6 h. (**F**) Time-course of the effect of PC(16:0/16:1 n − 7). The cells were incubated with the phospholipid (100 μM) for the indicated periods of time. The mRNA expression levels for *Il6* were analyzed by RT-qPCR. These data are given as means ± SD, n = 3; *** $p < 0.001$, significantly different from the corresponding LPS stimulations in the absence of added phospholipid, by one-way ANOVA followed by the Holm-Sidak test. (**G**) Effect of different stimuli on *Il6* expression. The cells were incubated with PC(16:0/16:1 n − 7) (green bars) or PC(16:0/16:1 n − 9) (red bars) or neither (open bars and blue bars) for 24 h. Afterward, they were stimulated with LPS (200 ng/ml), zymosan (500 μg/ml) or phorbol myristate acetate (PMA) (500 μg/ml) plus calcium ionophore A23185 (1 μM) as indicated for 6 h. Open bars denote incubations in the absence of stimulus. (**H**) Responses of TLR4-deficient cells. Cells were made deficient in TLR4 receptor expression by siRNA transfection. The cells were then treated as described in the experiment shown in panel G. These data (**G**, **H**) are given as means ± SD, n = 3; *** $p < 0.001$, significantly different from the corresponding stimulations in the absence of added phospholipid, by one-way ANOVA followed by the Holm-Sidak test. (**I-K**) The cells were treated as in panel **A** using 100 μM PC(16:0/16:1 n − 7) and stimulated by LPS for 4 h, as indicated. The mRNA expression levels for *Nlrp3* (**I**) and *Ilb* (**J**) were analyzed by RT-qPCR. These data are given as means ± SD, n = 5; ** $p < 0.01$, and *** $p < 0.001$, significantly different from the corresponding LPS stimulations in the absence of added phospholipid, by one-way ANOVA followed by the Holm-Sidak test. (**K**) The cells were treated as in panel **I** and the inflammasome was stimulated by treating with 5 mM ATP for 40 min. Cell supernatants were used for IL-1β quantification using specific ELISAs. These data are given as means ± SD, n = 4; ** $p < 0.01$, by one-way ANOVA followed by the Holm-Sidak test.

dependent responses were measured. *Il6* gene expression levels were assessed in these experiments. The PC(16:0/16:1 n − 7) effect was readily observable at concentrations as low as 25 μM and incubation times between 12 and 48 h (Fig. 3**E** and **F**). To assess whether the anti-inflammatory effect of PC(16:0/16:1 n − 7) is a general one on macrophage activation, other stimuli in addition to LPS, both receptor-directed (yeast-derived zymosan) and soluble (phorbol ester plus ionophore A23187), were tested. As shown in Fig. 3**G**, *Il6* gene expression was strongly reduced in the PC(16:0/16:1 n − 7)-treated cells under all activation conditions tested, demonstrating that the effect is general rather than stimulus-specific. PC(16:0/16:1 n − 9)-treated cells behaved similarly.

Given that LPS is a lipid ligand, it raises the possibility that the inhibitory effects observed with PC(16:0/16:1 n − 7) in the presence of LPS might stem, at least in part, from an interaction with TLR4, the receptor for LPS. To investigate this, we employed RAW264.7 macrophages in which TLR4 expression was silenced using siRNA. Previous studies, including our own, have shown that this approach consistently reduces TLR4 expression by more than 80 % in these cells [47–49]. As expected, LPS-induced *Il6* gene expression was nearly abolished (Fig. 3**H**). However, the cells responded normally to non-receptor-directed stimulation (PMA plus calcium ionophore) as well as to stimuli targeting other receptors (zymosan). In both cases, PC (16:0/16:1 n − 7) and PC(16:0/16:1 n − 9) blunted the responses to levels comparable to those observed in cells with intact TLR4 (*cf.* Fig. 3**G** and **H**). Thus, the inhibitory activity of PC(16:0/16:1 n − 7) is preserved in the absence of functional TLR4, indicating that its effects cannot be explained by direct competition for TLR4 binding or by ligand neutralization.

To extend our study to other inflammation-driven pathways, we next assessed the effect of PC(16:0/16:1 n − 7) on LPS-induced activation of the NLRP3 inflammasome and subsequent activation of IL-1β production. This is a key event in inflammatory signaling and autoimmune disease, driving immune responses and contributing to pathological inflammation [50–52]. PC(16:0/16:1 n − 7) markedly inhibited LPS-induced *Nlrp3* gene expression (Fig. 3**I**) as well as IL-1β production, both at the gene (Fig. 3**J**) and protein levels (Fig. 3**K**).

3.3. Liberation of free 16:1n−7 from PC(16:0/16:1n−7) is not required for the phospholipid to demonstrate anti-inflammatory activity

In activated cells, part of the 16:1 n − 7 present in PC is rapidly transferred to phosphatidylinositol (PI) through a Lands cycle-like deacylation/reacylation process initiated by the phospholipase iPLA$_2$β (group VIA calcium-independent phospholipase A$_2$) [23,24]. To investigate whether this 16:1 n − 7 remodeling pathway from PC to PI is relevant for the fatty acid to exert its anti-inflammatory effects, experiments were conducted in which the PC(16:0/16:1 n − 7)-loaded cells were exposed to LPS in the presence of two structurally unrelated iPLA$_2$β inhibitors, to prevent the movement of 16:1 n − 7 between phospholipid classes. The use of selective chemical inhibitors to investigate the role of intracellular PLA$_2$s during cell activation offers distinctive advantages, as chemical inhibition occurs rapidly, minimizing potential nonspecific effects that might develop over time. In addition, compensatory mechanisms that could complicate result interpretation do not come into play [53–55]. Moreover, chemical inhibitors specifically target PLA$_2$-dependent effects linked to enzymatic activity, while leaving noncatalytic functions of the enzyme unaffected [55,56]. The inhibitors used in this study were FKGK18 and BEL. FKGK18 is at least 200 times more potent at inhibiting iPLA$_2$β than other cellular PLA$_2$ forms [57] and has been shown to block iPLA$_2$β-mediated functions in cells and animal models of disease [58,59]. BEL shows strong selectivity for blocking Ca^{2+}-independent PLA$_2$ enzymes over Ca^{2+}-dependent ones in *in vitro* assays and whole cells, although it may also exert off-target effects depending on cell type [55,60]. Previously, we demonstrated that these two inhibitors completely block the transfer of 16:1 n − 7 from PC to PI in activated human monocytes and mouse peritoneal macrophages [23,24].

Fig. 4**A** shows that neither inhibitor exerted any effect on the reduced expression of the *Il6* gene by LPS in PC(16:0/16:1 n − 7)-loaded cells. In parallel experiments, we also tested the effect of triacsin C, an inhibitor of fatty acid reacylation reactions [61–63], which also blocks the transfer of 16:1 n − 7 from PC to PI in macrophages [24]. Triacsin C had no effect (Fig. 4**A**). These findings suggest that the anti-inflammatory effect of 16:1 n − 7-containing PC is unrelated to its hydrolysis by iPLA$_2$β leading to the liberation of free 16:1 n − 7. To further substantiate this view, we next examined the effect of reducing the expression levels of iPLA$_2$β on the LPS-induced responses. For these experiments, we used RAW264.7 macrophages and an iPLA$_2$β antisense oligonucleotide, which we and others have previously shown to strongly reduce iPLA$_2$β expression levels and activity [27,64]. Since we have consistently been unable to find reliable antibodies against murine iPLA$_2$β, the efficiency of antisense inhibition was assessed by determining mRNA levels by qPCR and by assaying the BEL-inhibitable iPLA$_2$ activity of cell homogenates after the different treatments. Using these procedures, we routinely achieved a 70 % decrease in iPLA$_2$β levels [23]. When challenged with LPS, both iPLA$_2$β-deficient and normal cells exhibited similar inhibitory responses to PC(16:0/16:1 n − 7), underscoring the lack of iPLA$_2$β involvement in this effect (Fig. 4**B**). Taken together, these data raise the key question of whether the anti-inflammatory properties of 16:1 n − 7 are conferred by the structural context of its integration into a specific phospholipid species. Seeking a definitive answer to this question, we went on to synthesize a PC molecule in which the 16:1 n − 7 lateral chain is linked to the glycerol backbone not by a

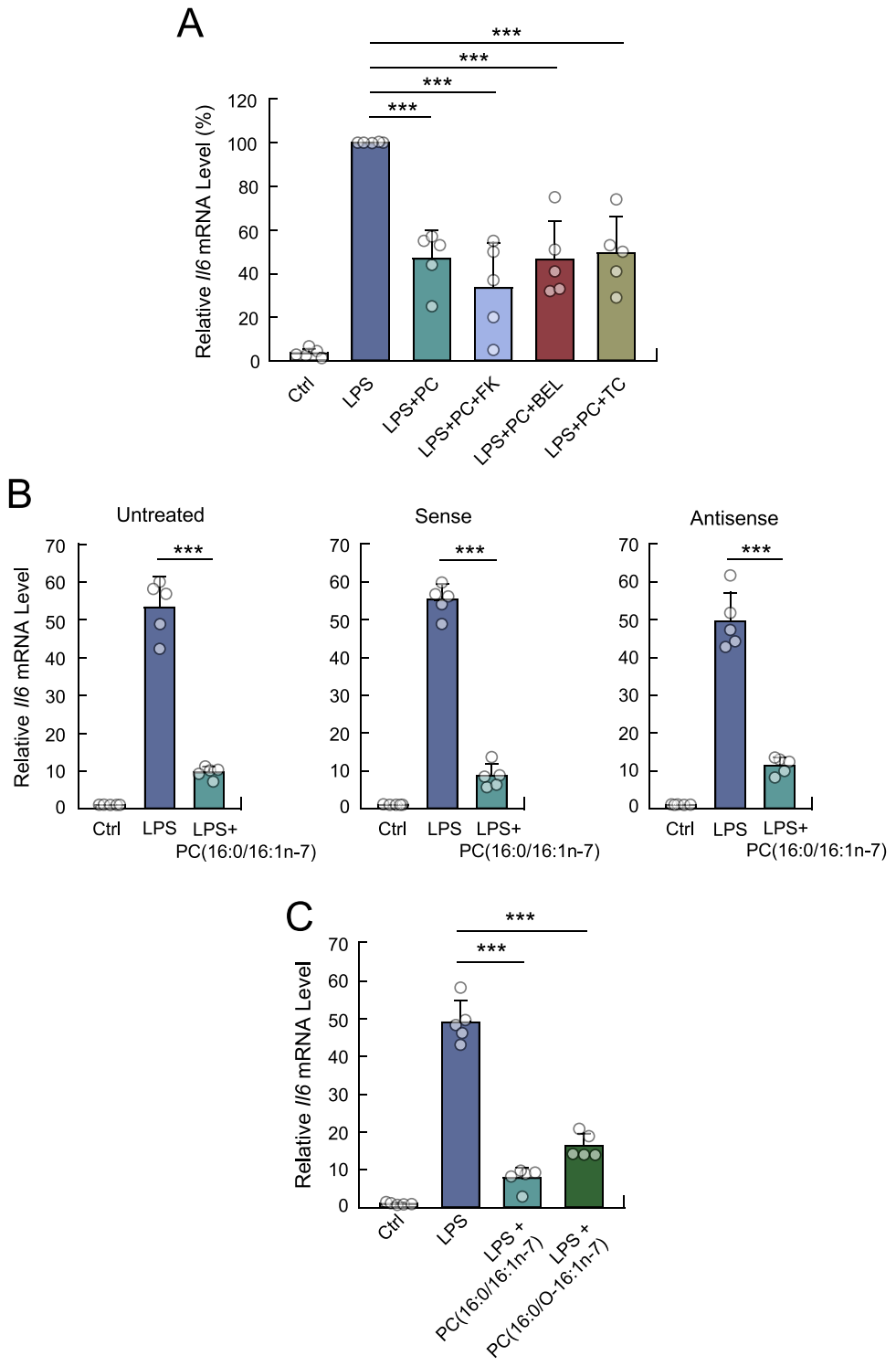

Fig. 4. The anti-inflammatory effects of PC(16:0/16:1 n − 7) reside in the whole phospholipid molecule and are independent of the liberation of free 16:1n–7. (**A**) The PC(16:0/16:1 n − 7)-loaded cells (abbreviated as PC in the figure) were stimulated with LPS in the presence of the iPLA$_2\beta$ inhibitors FKGK18 or BEL (both at 10 μM) or the acyl-CoA synthetase inhibitor triacsin C (TC) (3 μM), as indicated. The mRNA expression levels for *Il6* were analyzed by RT-qPCR. The data are given as means ± SD, n = 5. *** $p < 0.001$, significantly different from the LPS stimulations in the absence of added phospholipid, one-way ANOVA followed by the Holm-Sidak method. (**B**) The cells were treated for 24 h with 1 μM sense or antisense oligonucleotides or vehicle (Untreated), as indicated. Afterward the cells were loaded with PC(16:0/16:1 n − 7), and stimulated with LPS as indicated. The mRNA expression levels for *Il6* were analyzed by RT-qPCR. These data are given as means ± SD, n = 5. *** $p < 0.001$, significantly different from the LPS stimulations in the absence of added phospholipid, by Student's *t*-test. (**C**) The cells were incubated with the indicated phospholipid and, afterward, they were stimulated with 200 ng/ml LPS. *Il6* mRNA expression levels were analyzed by RT-qPCR. The results are shown as means ± SD, n = 5. *** $p < 0.001$, significantly different from the LPS stimulations in the absence of added phospholipid, by one-way ANOVA followed by the Holm-Sidak method.

classical ester bond but by an ether bond, PC(16:0/O-16:1 n − 7) (Fig. 1). This modification makes the phospholipid resistant to phospholipase attack and, hence, unable to release the 16:1 n − 7 moiety. The synthesis procedure for PC(16:0/O-16:1 n − 7) is available as Supplemental Material (Appendix B). The data shown in Fig. 4**C** demonstrate that, when used under identical conditions, both PC (16:0/16:1 n − 7) and the ether analog, PC(16:0/O-16:1 n − 7), inhibited the LPS-induced gene expression to comparable levels. These results show that the bioactive form of 16:1 n − 7 arises from its incorporation into a phospholipid rather than from the formation of a free fatty acid.

3.4. NF-κB p65 localization in cytoplasmic and nuclear compartments

Nuclear factor kappa B (NF-κB) plays a central role in regulating the transcription of pro-inflammatory genes in macrophages, thereby coordinating cellular responses to various stimuli such as pathogens, cytokines, and danger signals [65]. When activated, the p65/p50 heterodimer of NF-κB translocates to the nucleus, where it drives the expression of essential inflammatory genes [65]. As shown in Fig. 5**A** and **C**, treatment of cells with PC(16:0/16:1n–7) reduced their ability to induce nuclear translocation of NF-κB p65 between 1 and 3 h after LPS stimulation, as demonstrated by its detection in nuclear. To determine whether upstream events regulating NF-κB were also affected by the phospholipid, we analyzed the degradation and recovery of its inhibitor IκBα in cytosolic fractions from the same samples. Cells treated with PC (16:0/16:1n–7) demonstrated higher basal levels of IκBα (Fig. 5**B** and **D**). IκBα underwent a marked reduction after 1 h of LPS treatment; however, PC(16:0/16:1n–7)-treated cells maintained higher IκBα levels compared to controls. Importantly, recovery of IκBα, which largely depends on NF-κB activity [65], was delayed, an effect most evident at 6 h after LPS stimulation. Together, these findings show that PC (16:0/16:1n–7) increases NF-κB restriction prior to stimulation and limits its nuclear translocation and activity during stimulation.

In accordance with these data, immunofluorescence staining of NF-κB p65 in unstimulated macrophages showed a largely cytoplasmic location (Fig. 5**E**). Following treatment of the cells with LPS, the expected higher amounts of NF-κB p65 were readily found in nuclei. Importantly, the LPS-induced nuclear translocation of NF-κB p65 was strongly reduced in PC(16:0/16:1 n − 7)-loaded cells (Fig. 5**E**). These experiments were also conducted using the PC species containing hypogeic acid (16:1 n − 9) at the sn-2 position, and the same result was observed (Fig. 5**F**). This again indicated that the two 16:1 isomers possess comparable biological activity. Quantifications are shown in Figs. 5**G** and 5**H**.

Given that NF-κB is a hallmark of pro-inflammatory gene expression, we speculated that reduced activity of this transcription factor could conceivably skew the cells toward a more pronounced anti-inflammatory character [65]. In keeping with this idea, analyses of expression of the widely used markers for alternatively activated macrophages *Ym1* (*Chi3l3*) and *Fizz1* (*Retnla*) [66] were conducted by qPCR. Both markers were found to be markedly upregulated in the PC (16:0/16:1 n − 7)-loaded macrophages compared to untreated cells (Fig. 6**A** and **B**). For a more comprehensive characterization, we also employed the PC species containing 16:1 n − 9 in the sn-2 position, which produced the same results. In contrast, *Il10*, another anti-inflammatory gene, was unaffected (Fig. 6**C**). Note, however, that the LPS-induced up-regulation of this gene was further enhanced in the PC(16:0/16:1 n − 7)- or PC(16:0/16:1 n − 9)-loaded cells (Fig. 6**D**). Together, these results suggest that loading the macrophages with 16:1-containing PC intensifies their anti-inflammatory properties. To further characterize these PC(16:0/16:1 n − 7) effects, we conducted transcriptional mRNA profiling in murine macrophages under conditions that lead to an anti-inflammatory M2-like phenotype (IL-13 plus IL-4, 20 ng/ml, each for 12 h) [67]. To assess gene expression changes associated with M2 polarization, we analyzed a number of genes widely characterized to increase during M2 polarization [43] by RNAseq in cells incubated with or without phospholipid. The findings clearly demonstrated that both PC(16:0/16:1 n − 7) and PC(16:0/16:1 n − 9) substantially enhance the anti-inflammatory properties of macrophages by modulating gene expression patterns associated with alternative polarization (Fig. 6**E**). Flow cytometry analysis of CD206, the protein product of one of the genes appearing in Fig. 6E, *Mrc1*, demonstrated its expected increase in PC(16:0/16:1 n − 7)-treated cells compared to untreated cells (Fig. 6**F**).

3.5. Increased phagocytosis in macrophages loaded with 16:1-containing PC

Enhanced phagocytosis is a hallmark of alternatively activated (M2) macrophages, setting them apart from their pro-inflammatory counterparts [66,68]. Therefore, we next aimed to assess whether loading macrophages with 16:1-containing PC would induce a heightened phagocytic response. The 16:1-containing PC-loaded macrophages were exposed to fluorescent yeast-derived zymosan as a phagocytic challenge and analyzed by confocal microscopy. As in previous experiments, we utilized PC molecules containing either 16:1 n − 7 or 16:1 n − 9 at the *sn*-2 position. As shown in Fig. 7, cells loaded with both phospholipid species manifested a significantly enhanced phagocytic response. Importantly, parallel experiments using cells loaded with either PC (16:0/18:1 n − 9) or PC(16:0/16:0) showed no enhanced phagocytic activity compared to otherwise untreated control cells, thus highlighting the specificity of action of the 16:1 moiety (Fig. 7).

4. Discussion

Building on our previous work on lipid-mediated immune modulation [69,70], the current study sheds new light on the biological effects of 16:1 n − 7, highlighting its pivotal role in shaping macrophage responses to innate stimulation. Through multiple approaches, we provide evidence that the modulatory effects of 16:1 n − 7 on cytokine expression in activated macrophages and its general anti-inflammatory state are dependent upon its incorporation into a phospholipid. This observation is of interest, as it suggests a novel framework for understanding the effects of 16:1 n − 7 in inflammation; rather than the free fatty acid itself conveying the biological signal, it is a complex lipid metabolite, with the fatty acid incorporated into it, that drives the response.

When applied to cells, 16:1 n − 7 does not incorporate into a broad range of phospholipid species, as most other fatty acids do. Instead, it preferentially incorporates into a single species, namely PC(16:0/16:1) [22,23]. Given this specificity, it was reasonable to focus on this phospholipid species in our experiments. Moreover, employing a 16:1 n − 7-containing phospholipid instead of the free fatty acid represents a strategic approach with meaningful methodological advantages regarding the delivery of bioactive lipid principles into biological systems. Using the phospholipid species rather than the free fatty acid offers multiple benefits: (i) reduced toxicity, as free fatty acids are more cytotoxic at comparable concentrations; (ii) enhanced potency, since the phospholipid already constitutes the active principle, whereas free fatty acids must first incorporate into the appropriate phospholipid to exert their effects; and (iii) improved efficacy, ensuring that fatty acids are not wasted by becoming part of biologically inactive lipid species or used for β-oxidation. Finally, when considering delivery to whole organisms, phospholipids exhibit excellent biocompatibility and unique amphiphilic properties. These characteristics make them highly suitable for pharmaceutical applications [71,72].

Conversely, our work also anticipates that, beyond its regulatory actions shaping the macrophage inflammatory character, 16:1 n − 7-containing phospholipids may exert other functions in innate immune cells. This is based on our previous finding that 16:1 n − 7 incorporated into the cells as PC(16:0/16:1 n − 7), remains stable in this form if the cells are left otherwise untreated [22,23]. However, pro-inflammatory

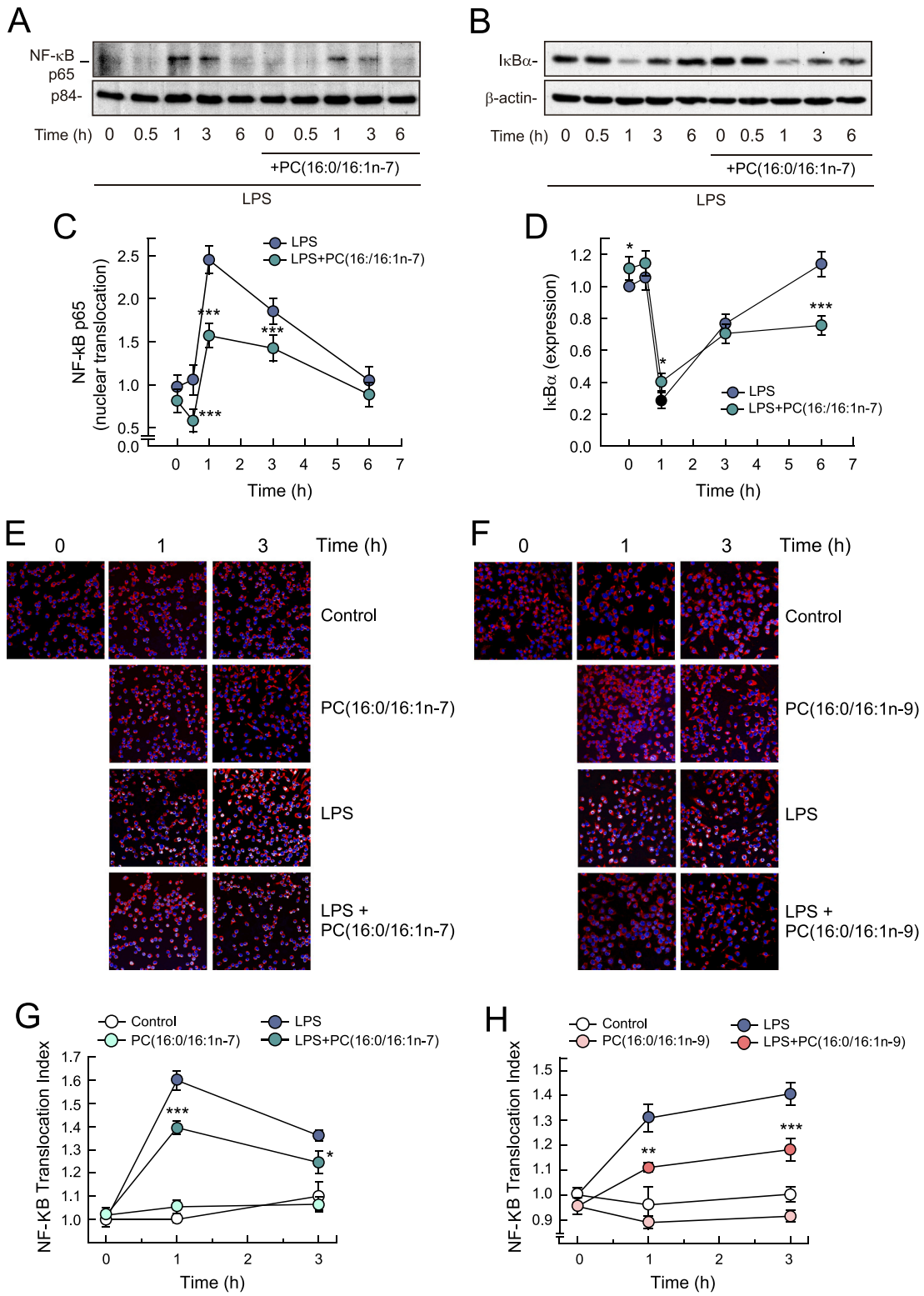

Fig. 5. PC(16:0/16:1 n − 7) and PC(16:0/16:1 n − 9) inhibit the LPS-induced nuclear translocation of NF-κB. (**A**, **B**) Cells were pretreated or not with PC(16:0/16:1 n − 7) as indicated and then stimulated with 200 ng/ml LPS for the indicated times. Nuclear and cytosolic fractions were prepared, and protein was analyzed by Western blot. (**A**) Nuclear NF-κB p65 was detected with specific antibodies, with p84 used as a loading control. (**B**) Cytosolic IκBα expression was analyzed using β-actin as a loading control. (**C**, **D**) Quantification of bands from panels **A** and **B**, normalized to protein levels at time zero. *$p < 0.05$, ***$p < 0.001$, significantly different between LPS and LPS plus PC(16:0/16:1 n − 7), by two-way ANOVA followed by the Holm–Sidak test. (**E**, **F**) The cells were pretreated or not (Control) with either PC(16:0/16:1 n − 7) (**E**) or PC(16:0/16:1 n − 9) (**F**), and then stimulated or not with 200 ng/ml LPS for the indicated periods of time. The cells were next inmunostained with antibodies against NF-κB p65 (red), and nuclei were stained with DAPI (blue). Subcellular localization of NF-κB p65 and DAPI was visualized by confocal microscopy, with colocalization shown in white. (**G**, **H**) Panels show the quantification of NF-κB p65 nuclear translocation with time, referred to the translocation level found in untreated control cells at time zero, which was taken as 1. The data are shown as means ± SD, n = 6. * $p < 0.05$, ** $p < 0.01$, and *** $p < 0.001$ significantly different LPS vs LPS plus PC(16:0/16:1 n − 7) or LPS plus PC(16:0/16:1 n − 9), by two-way ANOVA followed by the Holm-Sidak test.

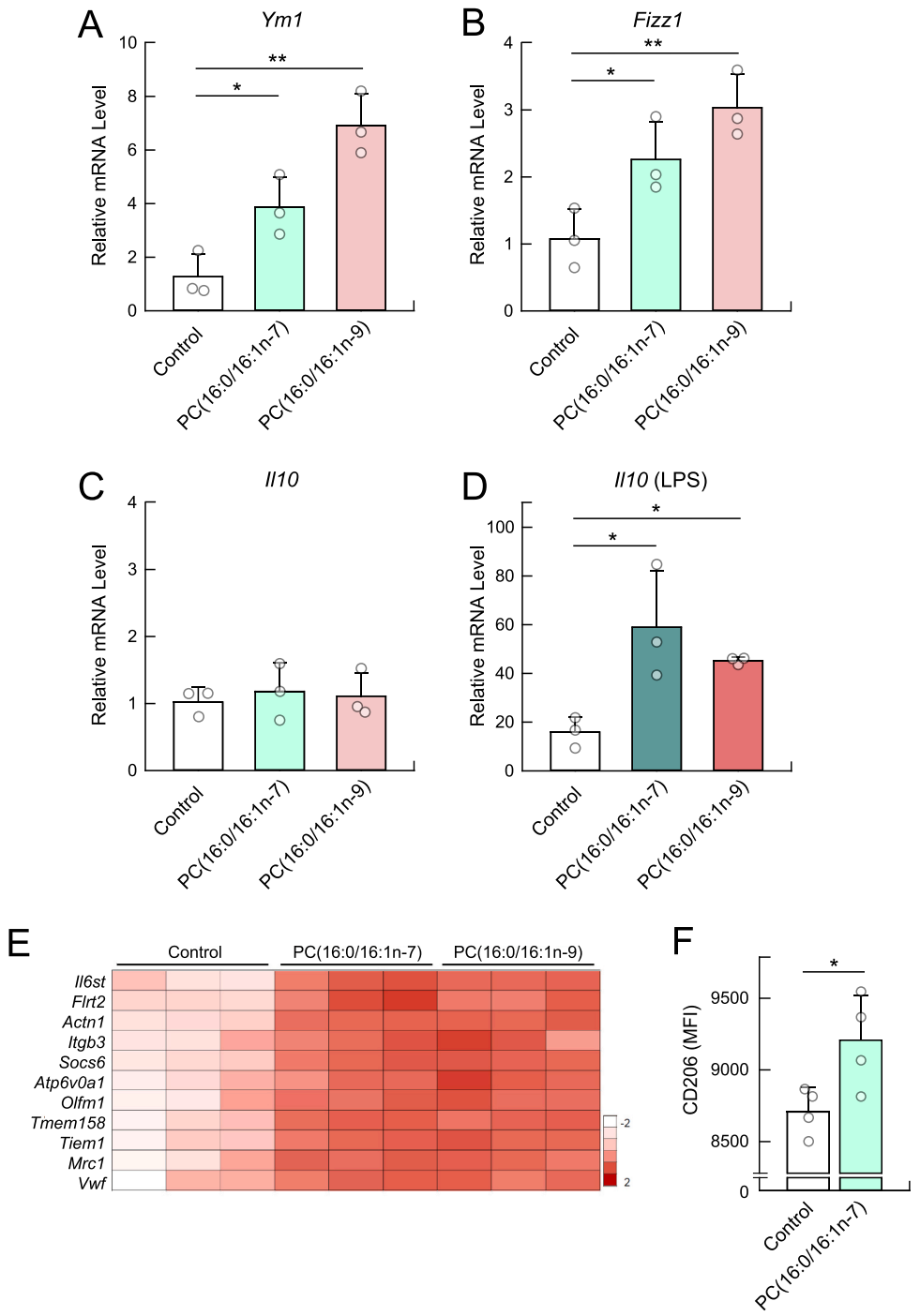

Fig. 6. PC(16:0/16:1 n − 7) and PC(16:0/16:1 n − 9) increase the expression of genes related to an anti-inflammatory phenotype. The cells were incubated with either PC(16:0/16:1 n − 7) (green bars) or PC(16:0/16:1 n − 9) (red bars) or left untreated (open bars) for 24 h. The mRNA expression levels for *Ym1* (**A**), *Fizz1* (**B**) and *Il10* (**C**) were then analyzed by RT-qPCR. Additionally, the phospholipid-loaded cells were stimulated with 200 ng/ml LPS and the *Il-10* mRNA expression levels were analyzed afterward (**D**). The results are shown as means ± SD, n = 3. * $p < 0.05$, and ** $p < 0.01$, significantly different from control conditions, by one-way ANOVA followed by the Holm-Sidak test. In other experiments, RNA expression levels of genes known to increase during macrophage polarization toward an anti-inflammatory M2 phenotype were analyzed by RNAseq from cells incubated or not with PC(16:0/16:1 n − 7) or PC(16:0/16:1 n − 9) (**E**). The heatmap represents the gene expression levels after Z-score transformation. Lower expression is represented by white, and higher expression by red. The color scale bar represents Z-score values. (**F**) Cells were incubated with PC(16:0/16:1 n − 7) or left untreated (Control) for 24 h, and CD206 expression was analyzed by flow cytometry. Mean fluorescence intensity (MFI) results are presented as means ± SD, n = 4. *$p < 0.05$, significantly different by Student's *t*-test.

activation of the cells with bacterial LPS or yeast-derived zymosan results in a fraction of the fatty acid being transferred from PC (16:0/16:1 n − 7) to a novel phospholipid species that did not exist before stimulation, or existed at very low levels, namely PI (18:0/16:1 n − 7). This remodeling reaction is mediated by the sequential actions of iPLA$_2$β, acyl-CoA synthetase, and CoA-dependent acyltransferases using the abundant lysoPI generated during macrophage activation as the acceptor [23,24]. Our data indicate that these interconnected reactions occur in parallel during activation but do not contribute to the anti-inflammatory effects of the fatty acid.

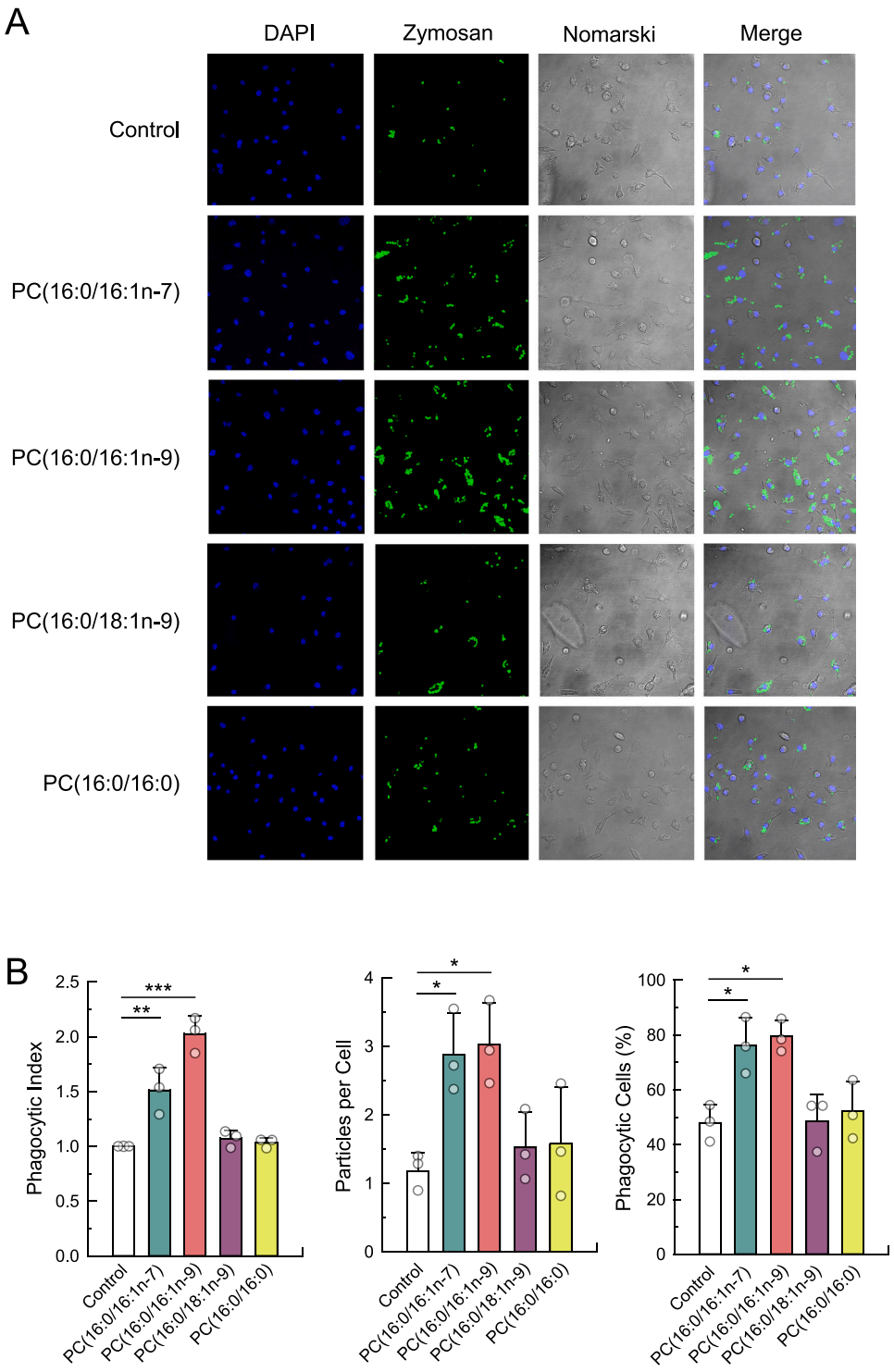

Fig. 7. Effect of different phospholipid molecular species on the phagocytosis of opsonized zymosan by murine peritoneal macrophages. Cells were incubated with the indicated phospholipids for 24 h. Afterward, fluorescent zymosan particles (10 particles per cell, equivalent to approximately 0.2 mg per million cells) were added for 60 min, and phagocytosis was analyzed by confocal microscopy (green color, second column from the left). DAPI (1 μg/ml) was used to mark the nuclei (blue; left column). Nomarski images (second column from the right) and the merge (right column) are also shown (**A**). Phagocytic index, number of particles per cell and the percentage of phagocytic cells of three independent experiments is shown in panel **B**. The data are shown as means ± SD, n = 3. Original magnification, × 20. * $p < 0.05$, ** $p < 0.01$, and *** $p < 0.001$, significantly different from the zymosan treatment in the absence of added phospholipid by one-way ANOVA followed by the Holm-Sidak test.

Transfer of fatty acyl moieties between phospholipids during cell activation is an integral component of lipid signaling, increasing phospholipid diversity and potentially generating unique lipid signatures, reflective of specific activation states in monocytes and macrophages. Moreover, the redistribution of 16:1 n − 7 among phospholipid classes could equip cells with novel or enhanced functional properties. Work in fibroblasts has suggested that the proliferative capacity of 16:1 n − 7 on various cell lines correlates with the enhanced production of a PI

molecule incorporating this fatty acid, thereby suggesting that this particular species might contribute to the growth-factor-like activity attributed to 16:1 n − 7 [73]. Likewise, previous work from our laboratory detected selective increases in 16:1-containing phospholipids in human monocytes activated by innate immune stimuli [74]. Collectively, these observations underscore the importance of defining and characterizing the metabolic pathways that govern cellular utilization of 16:1 n − 7 in order to fully elucidate its biological roles, including those underlying its anti-inflammatory effects and potentially other functions. In relation to the former, our results identify PC(16:0/16:1 n − 7) as a distinct phospholipid molecular species with intrinsic bioactivity, placing it among the expanding class of phospholipids that play specialized roles in stimulus–response coupling [75–80].

A possible explanation for the inhibitory effects of PC(16:0/16:1 n − 7) on LPS-induced responses could be that the phospholipid directly interferes with LPS binding to TLR4 or otherwise neutralizes the ligand. However, our experiments in TLR4-silenced macrophages argue against this interpretation. In these cells, LPS responses were nearly abolished as expected, yet PC(16:0/16:1 n − 7) continued to suppress responses to other stimuli, whether soluble (ionophore and phorbol ester) or those involving other surface receptors (zymosan). This finding indicates that the inhibitory effect of PC(16:0/16:1 n − 7) is not contingent upon the presence of TLR4 and is unlikely to be explained by simple LPS sequestration. Instead, the data are more consistent with a broader mechanism, such as modulation of membrane organization or downstream signaling components that can influence multiple receptor pathways converging on NF-κB. As a master regulator of the pro-inflammatory response of macrophages, NF-κB activation controls the expression of genes involved in immune activation, triggering the transcription of a number of pro-inflammatory cytokines that amplify the immune response, and promoting inflammation. Our results showing that cells treated with PC(16:0/16:1 n − 7) manifest a significantly reduced NF-κB activation provide a molecular frame to explain the strong anti-inflammatory character of this lipid, and its role in reprogramming the macrophage gene expression profile toward an anti-inflammatory M2 state.

Interestingly, the anti-inflammatory effects of PC(16:0/16:1 n − 7) are preserved when 16:1 n − 7 is replaced with its positional isomer 16:1 n − 9, but are lost when replaced with 18:1 n − 9. This finding aligns with observations by de Souza et al. [7], who reported that 16:1 n − 7, but not 18:1 n − 9, elicits significant anti-inflammatory responses in human endothelial cells. These results suggest that biological activity is dictated more by carbon number than by the position of the double bond relative to the methyl end. It is worth noting, however, that PC(16:0/18:1 n − 9) is known to possess biological activity in other settings, as this species has been described as an endogenous ligand of the nuclear receptor PPARα [75]. Research on PPARα ligands has shown inflammation reduction in several disease models, including allergic airway disease, arthritis, and inflammatory bowel disease [81]. Unlike these data, however, the anti-inflammatory effects of 16:1 n − 7 in liver have been shown to be completely independent of PPARα [8].

Another member of the PPAR family, PPARγ, has also been linked to the anti-inflammatory polarization of macrophages [82–84]. However, studies using cells from PPARγ-deficient mice failed to detect any effect of 16:1 n − 7 on macrophage responses [8], indicating that the 16:1 n − 7-induced effects are independent of this factor. Considering our own data, this is an interesting finding because some studies have demonstrated that PPARγ activation may inhibit NF-κB activation, thereby blunting the production of pro-inflammatory cytokines and chemokines [85,86]. Thus, the possibility that PC(16:0/16:1 n − 7) and PC(16:0/16:1 n − 9) suppress NF-κB via PPARγ-mediated mechanisms appears unlikely, as supported by the findings of Souza et al. [8].

Multiple non-exclusive mechanisms may account for the inhibition of NFκB signaling in macrophages by PC(16:0/16:1 n − 7), including direct molecular interactions with regulatory components or membrane-mediated modulation. The phospholipid species could act as a competitive ligand for lipid-binding domains in signaling proteins, altering their localization or conformation. In this regard, phosphatidylserine has been reported to suppress NF-κB activation in dendritic cells by preventing IκBα phosphorylation and degradation, thereby stabilizing cytoplasmic sequestration of NF-κB and preventing its nuclear translocation [87]. There is also evidence that certain phospholipids can activate phosphatases or inhibit kinases upstream of NF-κB, indirectly dampening the pathway. For example, the species PC (18:2/18:2) (1,2-dilinoleoyl-*sn*-glycero-3-phosphocholine) has been reported to block upstream MAPK activation and inhibit IκBα phosphorylation in neuronal cell models, thereby blunting NF-κB activation [88]. Notably, enriching macrophages with 16:1 n − 7, which, as previously noted, results in its pronounced accumulation in the species PC (16:0/16:1 n − 7), also leads to diminished MAPK activation [22].

On the other hand, defined PC and lysoPC species have been found to attenuate TNFα-induced NF-κB activation in epithelial cells, with efficacy correlated to unsaturation levels; that is, more unsaturated species exhibited stronger inhibitory effects [89]. This pattern underscores that lipid physicochemical properties, such as the degree of unsaturation, can significantly influence intracellular signaling. The effects may be mediated through changes in membrane architecture, particularly the organization of lipid rafts and other microdomains [90,91]. Such structural rearrangements can impact the spatial distribution and clustering of receptors, thereby altering the accessibility and activation of downstream signaling complexes like the IKK complex. Accordingly, 16:1-containing PC may exert its biological effects not only through structural integration but also by actively reshaping membrane architecture to influence signaling dynamics.

Pertinent to the results of this study, recent work has indicated that lysoPC molecules enriched with *cis* or *trans* 16:1 n − 7 isomers regulate insulin secretion from human EndoC-βH1 cells via activation of the GPR119 receptor, triggering cAMP-dependent signaling cascades [92]. Both isomers enhance glucose-stimulated insulin secretion [92,93] and regulate cholesterol metabolism [94], but they achieve this through different intracellular signaling pathways. These findings underscore the importance of lipid geometry and saturation in shaping molecular interactions and suggest that synthetic PCs, tailored with specific acyl chains, could be strategically designed to reorganize membrane microdomains and selectively modulate signaling pathways in metabolic disorders.

Macrophage differentiation and polarization are critically determined by the cellular environment, which also dictates cytokine responsiveness [95]. Our study emphasizes that the lipid composition may also critically affect the polarization state of the macrophage. Specifically, the incorporation of 16:1 n − 7 in PC shifts macrophage polarization in response to LPS by reducing pro-inflammatory cytokine production and enhancing the expression of M2-specific markers. In addition, given the ability of macrophages to repolarize [96], it is conceivable that 16:1 n − 7-containing PC also acts to hinder their transition between distinct polarization states, thereby preventing the adoption of an M1-like pro-inflammatory phenotype and its associated effector functions. This shift in macrophage polarization is recognized as a significant event in various pathophysiological settings, including tumorigenesis, wound healing, and inflammation resolution. Hence, its deregulation underlies both tumor progression and chronic inflammatory diseases [96,97]. Therefore, elucidating the mechanisms and molecular targets underlying the effects of 16:1 n − 7 may reveal novel opportunities for manipulating immune and inflammatory responses.

A logical consequence of the PC(16:0/16:1 n − 7)-driven shift of macrophages to an M2-like phenotype is their heightened phagocytic capacity. Again, this effect is similarly observed with PC molecules containing 16:1 n − 9 instead of 16:1 n − 7, but not when 18:1 n − 9 is used, highlighting 16:1 fatty acid specificity. In turn, this demonstrates that the enhancing effect of the 16:1 fatty acids is not merely due to the enrichment of membranes with monounsaturates that help maintain membrane fluidity [98], but may result from specific interactions

between 16:1 moieties and key molecular components. In this regard, we have previously demonstrated that a particular PLA_2 form, the secreted group V enzyme [99], is strongly upregulated in macrophages polarized to the M2 phenotype. This enzyme plays an active role in regulating the enhanced phagocytic response characteristic of these cells by modulating cellular lysophospholipid levels [99]. In intact cells, group V secreted PLA_2 preferentially hydrolyzes mono- and diunsaturated fatty acyl residues over polyunsaturated ones [100–103]. Studies are underway in our laboratory to determine whether macrophage loading with 16:1-containing PC molecules modulates group V PLA_2 activity, thereby influencing cellular lysophospholipid levels essential for sustaining the elevated phagocytic response of these cells.

In summary, the results of this study reveal that loading macrophages with 16:1-containing PC exerts protective effects against pro-inflammatory stimuli by reducing the production of cytokines through the inhibition of NF-κB activation. Ultimately, this process reprograms the gene expression profile, promoting an anti-inflammatory phenotype. The identification of broad gene expression changes induced by 16:1-containing PC highlights its potential to modulate macrophage responses in pathological conditions, reinforcing the therapeutic promise of defined synthetic PC species. Given their biocompatibility, chemical stability, and ability to integrate into lipid-based delivery systems such as liposomes and micelles, PC molecules are already employed in clinically successful nanoparticle platforms, including mRNA therapies [104,105]. However, their translational feasibility is challenged by rapid clearance, enzymatic degradation, and limited oral bioavailability. In systemic applications, circulating PC molecules, when part of liposomes or other nanocarriers, can form a protein corona that compromises vesicle stability and alters biodistribution [106]. Incorporating cholesterol has been shown to enhance bilayer robustness and reduce destabilization by plasma proteins [106,107], yet some liposomal formulations still risk complement activation–related pseudoallergy, leading to infusion reactions and immune responses [107]. Moreover, off-target effects and unintended membrane interactions remain concerns. Achieving clinical viability will require precise optimization of lipid composition, including PC species, PC-to-cholesterol ratio, and surface charge, alongside rigorous toxicological profiling to ensure stability, bioavailability, and safety.

Abbreviations

16:1 n − 7, palmitoleic acid (*cis*-9-hexadecenoic acid); 16:1 n − 9, hypogeic acid (*cis*-7-hexadecenoic acid); 18:1 n − 9, oleic acid (*cis*-9-octadecenoic acid); PLA_2, phospholipase A_2; $iPLA_2\beta$, group VIA calcium-independent phospholipase A_2; NF-κB, nuclear factor κB; LPS, bacterial lipopolysaccharide; PC, phosphatidylcholine; PE, phosphatidylethanolamine; PI, phosphatidylinositol.

CRediT authorship contribution statement

Jesús Balsinde: Writing – review & editing, Writing – original draft, Supervision, Project administration, Funding acquisition, Formal analysis, Conceptualization. **María A. Balboa:** Writing – review & editing, Writing – original draft, Supervision, Project administration, Funding acquisition, Formal analysis, Conceptualization. **Alfonso Pérez-Encabo:** Writing – review & editing, Supervision, Methodology, Investigation. **Miguel A. Bermúdez:** Writing – review & editing, Writing – original draft, Methodology, Investigation, Formal analysis. **Alvaro Garrido:** Methodology, Investigation. **Clara Meana:** Writing – review & editing, Methodology, Investigation, Formal analysis.

Declaration of Competing Interest

The authors declare that they have no known competing financial interests or personal relationships that could have appeared to influence the work reported in this paper.

Acknowledgments

We thank Montse Duque and Eva Merino for excellent technical assistance. This work was supported by grants PID2019–105989RB-I00 and PID2022-140764OB-I00, funded by the Spanish Ministry of Science, Innovation, and Universities, Agencia Estatal de Investigación (MICIN/AEI/10.13039/501100011033) and the European Union through the European Regional Development Fund, "A Way of Making Europe", and by grant CB07/08/0004 from CIBERDEM-Instituto de Salud Carlos III.

Appendix A. Supporting information

Supplementary data associated with this article can be found in the online version at doi:10.1016/j.biopha.2025.118652.

Data availability

Data will be made available on request.

References

[1] L. Schwingshackl, G. Hoffmann, Monounsaturated fatty acids, olive oil and health status: a systematic review and meta-analysis of cohort studies, Lipids Health Dis. 13 (2014) 154, https://doi.org/10.1186/1476-511X-13-154.
[2] C. Santa-María, S. López-Enríquez, S. Montserrat-de la Paz, I. Geniz, M.E. Reyes-Quiroz, M. Moreno, F. Palomares, F. Sobrino, G. Alba, Update on anti-inflammatory molecular mechanisms induced by oleic acid, Nutrients 15 (2023) 224, https://doi.org/10.3390/nu15010224.
[3] H. Cao, K. Gerhold, J.R. Mayers, M.M. Wiest, S.M. Watkins, G.S. Hotamisligil, Identification of a lipokine, a lipid hormone linking adipose tissue to systemic metabolism, Cell 134 (2008) 933–944, https://doi.org/10.1016/j.cell.2008.07.048.
[4] E. Erbay, V.R. Babaev, J.R. Mayers, L. Makowski, K.N. Charles, M.E. Snitow, S. Fazio, M.M. Wiest, S.M. Watkins, M.F. Linton, G.S. Hotamisligil, Reducing endoplasmic reticulum stress through a macrophage lipid chaperone alleviates atherosclerosis, Nat. Med. 15 (2009) 1383–1391, https://doi.org/10.1038/nm.2067.
[5] N.A. Talbot, C.P. Wheeler-Jones, M.E. Cleasby, Palmitoleic acid prevents palmitic acid-induced macrophage activation and consequent p38 MAPK-mediated skeletal muscle insulin resistance, Mol. Cell. Endocrinol. 393 (2014) 129–142, https://doi.org/10.1016/j.mce.2014.06.010.
[6] K.L. Chan, N.J. Pillon, D.M. Sivaloganathan, S.R. Costford, Z. Liu, M. Théret, B. Chazaud, A. Klip, Palmitoleate reverses high fat-induced pro-inflammatory macrophage polarization via AMP-activated protein kinase (AMPK), J. Biol. Chem. 290 (2015) 16979–16988, https://doi.org/10.1074/jbc.M115.646992.
[7] C.O. de Souza, C.A. Valenzuela, E.J. Baker, E.A. Miles, J.C. Rosa Neto, P. C. Calder, Palmitoleic acid has stronger anti-inflammatory potential in human endothelial cells compared to oleic and palmitic acids, Mol. Nutr. Food Res. 62 (2018) e1800322, https://doi.org/10.1002/mnfr.201800322.
[8] C.O. Souza, A.A.S. Teixeira, L.A. Biondo, L.S. Silveira, C.N. de Souza Breda, T. T. Braga, N.O.S. Camara, T. Belchior, W.T. Festuccia, T.A. Diniz, G.M. Ferreira, M. H. Hirata, A.B. Chaves-Filho, M.Y. Yoshinaga, S. Miyamoto, P.C. Calder, J. K. Sethi, J.C. Rosa Neto, Palmitoleic acid reduces high fat diet-induced liver inflammation by promoting PPAR-γ-independent M2a polarization of myeloid cells, Biochim. Biophys. Acta 1865 (2020) 158776, https://doi.org/10.1016/j.bbalip.2020.158776.
[9] M.M. Cruz, J.J. Simão, R. de Sá, T.S.M. Farias, V.S. da Silva, F. Abdala, V. J. Antraco, L. Armelin-Correa, M.I.C. Alonso-Vale, Palmitoleic acid decreases non-alcoholic hepatic steatosis and increases lipogenesis and fatty acid oxidation in adipose tissue from obese mice, Front. Endocrinol. 11 (2020) 537061, https://doi.org/10.3389/fendo.2020.537061.
[10] D. Tricò, A. Mengozzi, L. Nesti, M. Hatunic, R.G. Sánchez, T. Konrad, K. Lalić, N. M. Lalić, A. Mari, A. Natali, Circulating palmitoleic acid is an independent determinant of insulin sensitivity, beta cell function and glucose tolerance in non-diabetic individuals: a longitudinal analysis, Diabetologia 63 (2020) 206–218, https://doi.org/10.1007/s00125-019-05013-6.
[11] J. Gong, H. Campos, S. McGarvey, Z. Wu, R. Goldberg, A. Baylin, Adipose tissue palmitoleic acid and obesity in humans: does it behave as a lipokine? Am. J. Clin. Nutr. 93 (2011) 186–191, https://doi.org/10.3945/ajcn.110.006502.
[12] J.J. Lee, J.E. Lambert, Y. Hovhannisyan, M.A. Ramos-Roman, J.R. Trombold, D. A. Wagner, E.J. Parks, Palmitoleic acid is elevated in fatty liver disease and reflects hepatic lipogenesis, Am. J. Clin. Nutr. 101 (2015) 34–43, https://doi.org/10.3945/ajcn.114.092262.
[13] A. Samad, A. James, J. Wong, P. Mankad, J. Whitehouse, W. Patel, M. Alves-Simoes, A.K. Siriwardena, J.I. Bruce, Insulin protects pancreatic acinar cells from palmitoleic acid-induced cellular injury, J. Biol. Chem. 289 (2014) 23582–23595, https://doi.org/10.1074/jbc.M114.589440.
[14] Y. Akazawa, T. Morisaki, H. Fukuda, K. Norimatsu, J. Shiota, K. Hashiguchi, M. Tabuchi, M. Kitayama, K. Matsushima, N. Yamaguchi, H. Kondo, F. Fujita, H. Takeshita, K. Nakao, F. Takeshima, Significance of serum palmitoleic acid

levels in inflammatory bowel disease, Sci. Rep. 11 (2021) 16260, https://doi.org/10.1038/s41598-021-95923-6.
[15] E. Cetin, B. Pedersen, L.M. Porter, G.K. Adler, M.F. Burak, Protocol for a randomized placebo-controlled clinical trial using pure palmitoleic acid to ameliorate insulin resistance and lipogenesis in overweight and obese subjects with prediabetes, Front. Endocrinol. 14 (2023) 1306528, https://doi.org/10.3389/fendo.2023.1306528.
[16] E. De Fabiani, The true story of palmitoleic acid: between myth and reality, Eur. J. Lipid Sci. Technol. 113 (2011) 809–811, https://doi.org/10.1002/ejlt.201100187.
[17] L. Hodson, F. Karpe, Is there something special about palmitoleate? Curr. Opin. Clin. Nutr. Metab. Care 16 (2013) 225–231, https://doi.org/10.1097/MCO.0b013e32835d2edf.
[18] M.E. Frigolet, R. Gutiérrez-Aguilar, The role of the novel lipokine palmitoleic acid in health and disease, Adv. Nutr. 8 (2017) 173S–181S, https://doi.org/10.3945/an.115.011130.
[19] C.O. de Souza, G.K. Vannice, J.C. Rosa Neto, P.C. Calder, Is palmitoleic acid a plausible nonpharmacological strategy to prevent or control chronic metabolic and inflammatory disorders? Mol. Nutr. Food Res. 62 (2018) 1700504 https://doi.org/10.1002/mnfr.201700504.
[20] M.A. Bermúdez, L. Pereira, C. Fraile, L. Valerio, M.A. Balboa, J. Balsinde, Roles of palmitoleic acid and its positional isomers, hypogeic and sapienic acids, in inflammation, metabolic diseases and cancer, Cells 11 (2022) 2146, https://doi.org/10.3390/cells11142146.
[21] C. Guijas, C. Meana, A.M. Astudillo, M.A. Balboa, J. Balsinde, Foamy monocytes are enriched in cis-7-hexadecenoic fatty acid (16:1n-9), a possible biomarker for early detection of cardiovascular disease, Cell Chem. Biol. 23 (2016) 689–699, https://doi.org/10.1016/j.chembiol.2016.04.012.
[22] A.M. Astudillo, C. Meana, C. Guijas, L. Pereira, R. Lebrero, M.A. Balboa, J. Balsinde, Occurrence and biological activity of palmitoleic acid isomers in phagocytic cells, J. Lipid Res. 59 (2018) 237–249, https://doi.org/10.1194/jlr.M079145.
[23] A.M. Astudillo, C. Meana, M.A. Bermúdez, A. Pérez-Encabo, M.A. Balboa, J. Balsinde, Release of anti-inflammatory palmitoleic acid and its positional isomers by mouse peritoneal macrophages, Biomedicines 8 (2020) 480, https://doi.org/10.3390/biomedicines8110480.
[24] M.A. Bermúdez, A. Garrido, L. Pereira, T. Garrido, M.A. Balboa, J. Balsinde, Rapid movement of palmitoleic acid from phosphatidylcholine to phosphatidylinositol in activated human monocytes, Biomolecules 14 (2024) 707, https://doi.org/10.3390/biom14060707.
[25] J. Balsinde, B. Fernández, E. Diez, Regulation of arachidonic acid release in mouse peritoneal macrophages. The role of extracellular calcium and protein kinase c, J. Immunol. 144 (1990) 4298–4304, https://doi.org/10.4049/jimmunol.144.11.4298.
[26] A. Koeberle, H. Shindou, S.C. Koeberle, S.A. Laufer, T. Shimizu, O. Werz, Arachidonoyl-phosphatidylcholine oscillates during the cell cycle and counteracts proliferation by suppressing akt membrane binding, Proc. Natl. Acad. Sci. U. S. A. 110 (2013) 2546–2551, https://doi.org/10.1073/pnas.1216182110.
[27] J. Balsinde, M.A. Balboa, E.A. Dennis, Identification of a third pathway for arachidonic acid mobilization and prostaglandin production in activated P388D_1 macrophage-like cells, J. Biol. Chem. 275 (2000) 22544–22549, https://doi.org/10.1074/jbc.M910163199.
[28] J. Balsinde, M.A. Balboa, P.A. Insel, E.A. Dennis, Differential regulation of phospholipase d and phospholipase A_2 by protein kinase c in P388D_1 macrophages, Biochem. J. 321 (1997) 805–809, https://doi.org/10.1042/bj3210805.
[29] M.A. Balboa, R. Pérez, J. Balsinde, Amplification mechanisms of inflammation: paracrine stimulation of arachidonic acid mobilization by secreted phospholipase A_2 is regulated by cytosolic phospholipase A_2-derived hydroperoxyeicosatetraenoic acid, J. Immunol. 171 (2003) 989–994, https://doi.org/10.4049/jimmunol.171.2.989.
[30] M.A. Balboa, Y. Sáez, J. Balsinde, Calcium-independent phospholipase A_2 is required for lysozyme secretion in U937 promonocytes, J. Immunol. 170 (2003) 5276–5280, https://doi.org/10.4049/jimmunol.170.10.5276.
[31] M.M. Bradford, A rapid and sensitive method for the quantitation of microgram quantities of protein utilizing the principle of protein-dye binding, Anal. Biochem 72 (1976) 248–254, https://doi.org/10.1016/0003-2697(76)90527-3.
[32] J. Pindado, J. Balsinde, M.A. Balboa, TLR3-dependent induction of nitric oxide synthase in RAW 264.7 macrophage-like cells via a cytosolic phospholipase A_2/cyclooxygenase-2 pathway, J. Immunol. 179 (2007) 4821–4828, https://doi.org/10.4049/jimmunol.179.7.4821.
[33] V. Ruipérez, M.A. Astudillo, M.A. Balboa, J. Balsinde, Coordinate regulation of TLR-mediated arachidonic acid mobilization in macrophages by group IVA and group v phospholipase A_2s, J. Immunol. 182 (2009) 3877–3883, https://doi.org/10.4049/jimmunol.0804003.
[34] E.G. Bligh, W.J. Dyer, A rapid method of total lipid extraction and purification, Can. J. Biochem. Physiol. 37 (1959) 911–917, https://doi.org/10.1139/o59-099.
[35] E. Diez, J. Balsinde, M. Aracil, A. Schüller, Ethanol induces release of arachidonic acid but not synthesis of eicosanoids in mouse peritoneal macrophages, Biochim. Biophys. Acta 921 (1987) 82–89, https://doi.org/10.1016/0005-2760(87)90173-1.
[36] J.B. Fine, H. Sprecher, Unidimensional thin-layer chromatography of phospholipids on boric acid-impregnated plates, J. Lipid Res. 23 (1982) 660–663, https://doi.org/10.1016/S0022-2275(20)38132-3.
[37] K.J. Livak, T.D. Schmittgen, Analysis of relative gene expression data using real-time quantitative PCR and the $2^{-\Delta\Delta\ Ct}$ method, Methods 25 (2001) 402–408, https://doi.org/10.1006/meth.2001.1262.
[38] A. Dobin, C.A. Davis, F. Schlesinger, J. Drenkow, C. Zaleski, S. Jha, P. Batut, M. Chaisson, T.R. Gingeras, STAR: ultrafast universal RNA-seq aligner, Bioinformatics 29 (2013) 15–21, https://doi.org/10.1093/bioinformatics/bts635.
[39] Y. Liao, G.K. Smyth, W. Shi, Featurecounts: an efficient general purpose program for assigning sequence reads to genomic features, Bioinformatics 30 (2014) 923–930, https://doi.org/10.1093/bioinformatics/btt656.
[40] M.D. Robinson, D.J. McCarthy, G.K. Smyth, Edger: a bioconductor package for differential expression analysis of digital gene expression data, Bioinformatics 26 (2010) 139–140, https://doi.org/10.1093/bioinformatics/btp616.
[41] C.W. Law, Y. Chen, W. Shi, G.K. Smyth, Voom: precision weights unlock linear model analysis tools for RNA-seq read counts, Genome Biol. 15 (2014) R29, https://doi.org/10.1186/gb-2014-15-2-r29.
[42] S. Zhao, Y. Guo, Q. Sheng, Y. Shyr, Heatmap3: an improved heatmap package with more powerful and convenient features, BMC Bioinforma. 15 (2014) P16, https://doi.org/10.1186/1471-2105-15-S10-P16.
[43] K.A. Jablonski, S.A. Amici, L.M. Webb, J.D. Ruiz-Rosado, P.G. Popovich, P. Partida-Sanchez, M. Guerau-de-Arellano, Novel markers to delineate murine M1 and M2 macrophages, PLoS One 10 (2015) e0145342, https://doi.org/10.1371/journal.pone.0145342.
[44] M. Girotti, J.H. Evans, D. Burke, C.C. Leslie, Cytosolic phospholipase A_2 translocates to forming phagosomes during phagocytosis of zymosan in macrophages, J. Biol. Chem. 279 (2004) 19113–19121, https://doi.org/10.1074/jbc.M313867200.
[45] B. Balestrieri, V.,W. Hsum, H. Gilbert, C.C. Leslie, W.K. Han, J.V. Bonventre, J. V. Arm, Group v secretory phospholipase A_2 translocates to the phagosome after zymosan stimulation of mouse peritoneal macrophages and regulates phagocytosis, J. Biol. Chem. 281 (2006) 6691–6698, https://doi.org/10.1074/jbc.M508314200.
[46] B. Balestrieri, A. Maekawa, W. Xing, M.H. Gelb, H.R. Katz, J.P. Arm, Group v secretory phospholipase A_2 modulates phagosome maturation and regulates the innate immune response against *candida albicans*, J. Immunol. 182 (2009) 4891–4898, https://doi.org/10.4049/jimmunol.0803776.
[47] X. Hu, J. Zhou, S. Song, W. Kong, Y.C. Shi, L.L. Chen, T.S. Zeng, TLR4/AP-1-targeted anti-inflammatory intervention attenuates insulin sensitivity and liver steatosis, Mediat. Inflamm. 2020 (2020) 2960517, https://doi.org/10.1155/2020/2960517.
[48] Z. Xu, C.X. Huang, Y. Li, P.Z. Wang, G.L. Ren, C.S. Chen, F.J. Shang, Y. Zhang, Q. Q. Liu, Z.S. Jia, Q.H. Nie, Y.T. Sun, X.F. Bai, Toll-like receptor 4 siRNA attenuates LPS-induced secretion of inflammatory cytokines and chemokines by macrophages, J. Infect. 55 (2007) e1–e9, https://doi.org/10.1016/j.jinf.2007.01.003.
[49] M. Aoki, T. Ishii, M. Kanaoka, T. Kimura, RNA interference in immune cells by use of osmotic delivery of siRNA, Biochem. Biophys. Res. Commun. 341 (2006) 326–333, https://doi.org/10.1016/j.bbrc.2005.12.191.
[50] Y. Chen, X. Ye, G. Escames, W. Lei, X. Zhang, M. Li, T. Jing, Y. Yao, Z. Qiu, Z. Wang, D. Acuña-Castroviejo, Y. Yang, The NLRP3 inflammasome: contributions to inflammation-related diseases, Cell. Mol. Biol. Lett. 28 (2023) 51, https://doi.org/10.1186/s11658-023-00462-9.
[51] Y. Zhang, W. Yang, W. Li, Y. Zhao, NLRP3 inflammasome: checkpoint connecting innate and adaptive immunity in autoimmune diseases, Front. Immunol. 12 (2021) 732933, https://doi.org/10.3389/fimmu.2021.732933.
[52] H. Guo, J.B. Callaway, J.P.Y. Ting, Inflammasomes: mechanism of action, role in disease, and therapeutics, Nat. Med. 21 (2015) 677–687, https://doi.org/10.1038/nm.3893.
[53] L. Gil-de-Gómez, A.M. Astudillo, C. Guijas, V. Magrioti, G. Kokotos, M.A. Balboa, J. Balsinde, Cytosolic group IVA and calcium-independent group VIA phospholipase A_2s act on distinct phospholipid pools in zymosan-stimulated mouse peritoneal macrophages, J. Immunol. 192 (2014) 752–762, https://doi.org/10.4049/jimmunol.1302267.
[54] P. Lebrero, A.M. Astudillo, J.M. Rubio, L. Fernández-Caballero, G. Kokotos, M. A. Balboa, J. Balsinde, Cellular plasmalogen content does not influence arachidonic acid levels or distribution in macrophages: a role for cytosolic phospholipase A_2 in phospholipid remodeling, Cells 8 (2019) 799, https://doi.org/10.3390/cells8080799.
[55] E.A. Dennis, J. Cao, Y.H. Hsu, V. Magrioti, G. Kokotos, Phospholipase A_2 enzymes: physical structure, biological function, disease implication, chemical inhibition, and therapeutic intervention, Chem. Rev. 111 (2010) 6130–6185, https://doi.org/10.1021/cr200085w.
[56] A. Nikolaou, M.G. Kokotou, S. Vasilakaki, G. Kokotos, Small-molecule inhibitors as potential therapeutics and as tools to understand the role of phospholipases A_2, Biochim. Biophys. Acta 1864 (2019) 941–956, https://doi.org/10.1016/j.bbalip.2018.08.009.
[57] G. Kokotos, Y.H. Hsu, J.E. Burke, C. Baskakis, C.G. Kokotos, V. Magrioti, E. A. Dennis, Potent and selective fluoroketone inhibitors of group VIA calcium-independent phospholipase A_2, J. Med. Chem. 53 (2010) 3602–3610, https://doi.org/10.1021/jm901872v.
[58] C. Dedaki, M.G. Kokotou, V.D. Mouchlis, D. Limnios, X. Lei, C.T. Mu, S. Ramanadham, V. Magrioti, E.A. Dennis, G. Kokotos, β-Lactones: a novel class of Ca^{2+}-independent phospholipase A_2 (group VIA iPLA_2) inhibitors with the ability to inhibit β-cell apoptosis, J. Med. Chem. 62 (2019) 2916–2927, https://doi.org/10.1021/acs.jmedchem.8b01216.

[59] R.N. Bone, Y. Gai, V. Magrioti, M.G. Kokotou, T. Ali, X. Lei, H.M. Tse, G. Kokotos, S. Ramanadham, Inhibition of Ca^{2+}-independent phospholipase A_2 (iPLA$_2\beta$) ameliorates islet infiltration and incidence of diabetes in NOD mice, Diabetes 64 (2015) 541–554, https://doi.org/10.2337/db14-0097.

[60] S. Ramanadham, T. Ali, J.W. Ashley, R.N. Bone, W.D. Hancock, X. Lei, Calcium-independent phospholipases A_2 and their roles in biological processes and diseases, J. Lipid Res. 56 (2015) 1643–1668, https://doi.org/10.1194/jlr.R058701.

[61] E.J. Hartman, S. Omura, M. Laposata, Triacsin C: a differential inhibitor of arachidonoyl-CoA synthetase and nonspecific long chain acyl-CoA synthetase, Prostaglandins 37 (1989) 655–671, https://doi.org/10.1016/0090-6980(89)90103-2.

[62] J.H. Kim, T.M. Lewin, R.A. Coleman, Expression and characterization of recombinant rat acyl-CoA synthetases 1, 4, and 5. Selective inhibition by triacsin c and thiazolidinediones, J. Biol. Chem. 276 (2001) 24667–24673, https://doi.org/10.1074/jbc.M010793200.

[63] D.A. Vessey, M. Kelley, R.S. Warren, Characterization of triacsin c inhibition of short-, medium-, and long-chain fatty acid: CoA ligases of human liver, J. Biochem. Mol. Toxicol. 18 (2004) 100–106, https://doi.org/10.1002/jbt.20009.

[64] K.A. Carnevale, M.K. Cathcart, Calcium-independent phospholipase A2 is required for human monocyte chemotaxis to monocyte chemoattractant protein 1, J. Immunol. 167 (2001) 3414–3421, https://doi.org/10.4049/jimmunol.167.6.3414.

[65] L. Barnabei, E. Laplantine, W. Mbongo, F. Rieux-Laucat, R. Weil, NF-κB: at the borders of autoimmunity and inflammation, Front. Immunol. 12 (2021) 716469, https://doi.org/10.3389/fimmu.2021.716469.

[66] S. Gordon, F.O. Martinez, Alternative activation of macrophages: mechanism and functions, Immunity 32 (2010) 593–604, https://doi.org/10.1016/j.immuni.2010.05.007.

[67] J.C. Rodríguez-Prados, P.G. Través, J. Cuenca, D. Rico, J. Aragonés, P. Martín-Sanz, M. Cascante, L. Boscá, Substrate fate in activated macrophages: a comparison between innate, classic, and alternative activation, J. Immunol. 185 (2010) 605–614, https://doi.org/10.4049/jimmunol.0901698.

[68] C. Rosales, E. Uribe-Querol, Phagocytosis: a fundamental process in immunity, BioMed. Res. Int. 2017 (2017) 9042851, https://doi.org/10.1155/2017/9042851.

[69] A.M. Astudillo, M.A. Balboa, J. Balsinde, Compartmentalized regulation of lipid signaling in oxidative stress and inflammation: plasmalogens, oxidized lipids and ferroptosis as new paradigms of bioactive lipid research, Prog. Lipid Res. 89 (2023) 101207, https://doi.org/10.1016/j.plipres.2022.101207.

[70] J.P. Rodríguez, J. Casas, M.A. Balboa, J. Balsinde, Bioactive lipid signaling and lipidomics in macrophage polarization: impact on inflammation and immune regulation, Front. Immunol. 16 (2025) 1550500, https://doi.org/10.3389/fimmu.2025.1550500.

[71] J. Li, X. Wang, T. Zhang, C. Vang, Z. Huang, X. Luo, Y. Deng, A review on phospholipids and their main applications in druge delivery systems, Asian J. Pharm. Sci. 10 (2015) 81–98, https://doi.org/10.1016/j.ajps.2014.09.004.

[72] G. Fricker, T. Kromp, A. Wender, A. Blume, J. Zirkel, H. Rebmann, C. Setzer, R. O. Quinkert, F. Martin, C. Müller-Goymann, Phospholipids and lipid-based formulations in oral drug delivery, Pharm. Res. 27 (2010) 1469–1486, https://doi.org/10.1007/s11095-010-0130-x.

[73] A. Koeberle, H. Shindou, T. Harayama, T. Shimizu, Palmitoleate is a mitogen, formed upon stimulation with growth factors, and converted to palmitoleoyl-phosphatidylinositol, J. Biol. Chem. 287 (2012) 27244–27254, https://doi.org/10.1074/jbc.M111.274829.

[74] D. Balgoma, A.M. Astudillo, G. Pérez-Chacón, O. Montero, M.A. Balboa, J. Balsinde, Markers of monocyte activation revealed by lipidomic profiling of arachidonic acid-containing phospholipids, J. Immunol. 184 (2010) 3857–3865, https://doi.org/10.4049/jimmunol.0902883.

[75] M.V. Chakravarthy, I.J. Lodhi, L. Yin, R.R. Malapaka, H.E. Xu, J. Turk, C. F. Semenkovich, Identification of a physiologically relevant endogenous ligand for PPARα in liver, Cell 138 (2009) 476–488, https://doi.org/10.1016/j.cell.2009.05.036.

[76] M.A. Balboa, J. Balsinde, D.A. Dillon, G.M. Carman, E.A. Dennis, Proinflammatory macrophage-activating properties of the novel phospholipid diacylglycerol pyrophosphate, J. Biol. Chem. 274 (1999) 522–526, https://doi.org/10.1074/jbc.274.1.522.

[77] Y. Shirai, J. Balsinde, E.A. Dennis, Localization and functional interrelationships among cytosolic group IV, secreted group V, and Ca^{2+}-independent group VI phospholipase A_2s in P388D_1 macrophages using GFP/RFP constructs, Biochim. Biophys. Acta 1735 (2005) 119–129, https://doi.org/10.1016/j.bbalip.2005.05.005.

[78] J.M. Lee, Y.K. Lee, J.L. Mamrosh, S.A. Busby, P.R. Griffin, M.C. Pathak, E. A. Ortlund, D.D. Moore, A nuclear receptor-dependent phosphatidylcholine pathway with antidiabetic effects, Nature 474 (2011) 506–510, https://doi.org/10.1038/nature10111.

[79] V.B. O'Donnell, R.C. Murphy, New families of bioactive oxidized phospholipids generated by immune cells: identification and signaling actions, Blood 120 (2012) 1985–1992, https://doi.org/10.1182/blood-2012-04-402826.

[80] M. Thürmer, A. Gollowitzer, H. Pein, K. Neukirch, E. Gelmez, L. Waltl, N. Wielsch, R. Winkler, K. Löser, J. Grander, et al., PI(18:1/18:1) is a SCD1-derived lipokine that limits stress signaling, Nat. Commun. 13 (2022) 2982, https://doi.org/10.1038/s41467-022-30374-9.

[81] D.S. Straus, C.K. Glass, Anti-inflammatory actions of PPAR ligands: new insights on cellular and molecular mechanisms, Trends Immunol. 28 (2007) 551–558, https://doi.org/10.1016/j.it.2007.09.003.

[82] R. Stienstra, C. Duval, S. Keshtkar, J. van der Laak, S. Kersten, M. Muller, Peroxisome proliferator-activated receptor gamma activation promotes infiltration of alternatively activated macrophages into adipose tissue, J. Biol. Chem. 283 (2008) 22620–22627, https://doi.org/10.1074/jbc.M710314200.

[83] L.S. Silveira, H.A.P. H.A.P. Batatinha, A. Castoldi, N.O.S. Camara, W.T. Festuccia, C.O. Souza, J.C. Rosa Neto, F.S. Lira, Exercise rescues the immune response fine-tuned impaired by peroxisome proliferator-activated receptors gamma deletion in macrophages, J. Cell. Physiol. 234 (2019) 5241–5251, https://doi.org/10.1002/jcp.27333.

[84] X. Prieur, C.Y. Mok, V.R. Velagapudi, V. Nunez, L. Fuentes, D. Montaner, K. Ishikawa, A. Camacho, N. Barbarroja, S. O'Rahilly, J.K. Sethi, J. Dopazo, M. Oresic, M. Ricote, A. Vidal-Puig, Differential lipid partitioning between adipocytes and tissue macrophages modulates macrophage lipotoxicity and M2/M1 polarization in obese mice, Diabetes 60 (2011) 797–809, https://doi.org/10.2337/db10-0705.

[85] A. Croasdell, P.F. Duffney, N. Kim, S.H. Lacy, P.J. Sime, R.,P. Phipps, PPARγ and the innate immune system mediate the resolution of inflammation, PPAR Res 2015 (2015) 549691, https://doi.org/10.1155/2015/549691.

[86] M.R. Jain, S.R. Giri, B. Bhoi, C. Trivedi, A. Rath, R. Rathod, R. Ranvir, S. Kadam, H. Patel, P. Swain, S.S. Roy, N. Das, E. Karmakar, W. Wahli, P.R. Patel, Dual PPARα/γ agonist saroglitazar improves liver histopathology and biochemistry in experimental NASH models, Liver Int 38 (2018) 1084–1094, https://doi.org/10.1111/liv.13634.

[87] K. Doffek, X. Chen, S.L. Sugg, J. Shilyansky, Phosphatidylserine inhibits NFκB and p38 MAPK activation in human monocyte derived dendritic cells, Mol. Immunol. 48 (2011) 1771–1777, https://doi.org/10.1016/j.molimm.2011.04.021.

[88] N.R. Pandey, K. Sultan, E. Twomey, D.L. Sparks, Phospholipids block nuclear factor-kappa b and tau phosphorylation and inhibit amyloid-beta secretion in human neuroblastoma cells, Neuroscience 164 (2009) 1744–1753, https://doi.org/10.1016/j.neuroscience.2009.09.062.

[89] I. Treede, A. Braun, P. Jeliaskova, T. Giese, J. Füllekrug, G. Griffiths, W. Stremmel, R. Ehehalt, TNF-alpha-induced up-regulation of pro-inflammatory cytokines is reduced by phosphatidylcholine in intestinal epithelial cells, BMC Gastroenterol. 9 (2009) 53, https://doi.org/10.1186/1471-230x-9-53.

[90] M. Warda, S. Tekin, M. Gamal, N. Khafaga, F. Çelebi, G. Tarantino, Lipid rafts: novel therapeutic targets for metabolic, neurodegenerative, oncological, and cardiovascular diseases, Lipids Health Dis. 24 (2025) 147, https://doi.org/10.1186/s12944-025-02563-0.

[91] P. Varshney, V. Yadav, N. Saini, Lipid rafts in immune signalling: current progress and future perspective, Immunology 149 (2016) 13–24, https://doi.org/10.1111/imm.12617.

[92] M. Szustak, E. Korkus, R. Madaj, A. Chworos, G. Dąbrowski, S. Czaplicki, E. Tabandeh, G. Maciejewska, M. Koziołkiewicz, I. Konopka, A. Gliszczyńska, E. Gendaszewska-Darmach, Lysophosphatidylcholines enriched with cis and trans palmitoleic acid regulate insulin secretion via GPR119 receptor, ACS Med. Chem. Lett. 15 (2024) 197–204, https://doi.org/10.1021/acsmedchemlett.3c00263.

[93] E. Korkus, M. Szustak, R. Madaj, A. Chworos, A. Drzazga, M. Koziołkiewicz, G. Dąbrowski, S. Czaplicki, I. Konopka, E. Gendaszewska-Darmach, Trans-palmitoleic acid, a dairy fat biomarker, stimulates insulin secretion and activates g protein-coupled receptors with a different mechanism from the cis isomer, Food Funct. 14 (2023) 6496–6512, https://doi.org/10.1039/d2fo03412c.

[94] W. Huang, B. Hong, K. Bai, R. Tan, T. Yang, J. Sun, R. Yi, H. Wu, Cis- and trans-palmitoleic acid isomers regulate cholesterol metabolism in different ways, Front. Pharm. 11 (2020) 602115, https://doi.org/10.3389/fphar.2020.602115.

[95] E. Sierra-Filardi, A. Puig-Kröger, F.J. Blanco, C. Nieto, R. Bragado, M.I. Palomero, C. Bernabeu, M.A. Vega, A.L. Corbí, Activin a skews macrophage polarization by promoting a proinflammatory phenotype and inhibiting the acquisition of anti-inflammatory macrophage markers, Blood 117 (2011) 5092–5101, https://doi.org/10.1182/blood-2010-09-306993.

[96] P. Allavena, A. Sica, C. Garlanda, A. Mantovani, The yin-yang of tumor-associated macrophages in neoplastic progression and immune surveillance, Immunol. Rev. 222 (2008) 155–161, https://doi.org/10.1111/j.1600-065X.2008.00607.x.

[97] J.M. Olefsky, C.K. Glass, Macrophages, inflammation, and insulin resistance, Annu Rev. Physiol. 72 (2010) 219–246, https://doi.org/10.1146/annurev-physiol-021909-135846.

[98] J. Schumann, It is all about fluidity: fatty acids and macrophage phagocytosis, Eur. J. Pharm. 785 (2016) 18–23, https://doi.org/10.1016/j.ejphar.2015.04.057.

[99] J.M. Rubio, J.P. Rodríguez, L. Gil-de-Gómez, C. Guijas, M.A. Balboa, J. Balsinde, Group v secreted phospholipase A_2 is up-regulated by interleukin-4 in human macrophages and mediates phagocytosis via hydrolysis of ethanolamine phospholipids, J. Immunol. 194 (2015) 3327–3339, https://doi.org/10.4049/jimmunol.1401026.

[100] J. Balsinde, M.A. Balboa, S. Yedgar, E.A. Dennis, Group v phospholipase A_2-mediated oleic acid mobilization in lipopolysaccharide-stimulated P388D_1 macrophages, J. Biol. Chem. 275 (2000) 4783–4786, https://doi.org/10.1074/jbc.275.7.4783.

[101] K. Watanabe, Y. Taketomi, Y. Miki, K. Kugiyama, M. Murakami, Group v secreted phospholipase A_2 plays a protective role against aortic dissection, J. Biol. Chem. 295 (2020) 10092–10111, https://doi.org/10.1074/jbc.RA120.013753.

[102] M. Sendetski, S. Wedel, K. Furutani, L. Hahnefeld, C. Angioni, J. Heering, B. Zimmer, S. Pierre, A.M. Banica, K. Scholich, S. Tunaru, G. Geisslinger, R.R. Ji, M. Sisignano, Oleic acid released by sensory neurons inhibits TRPV1-mediated

thermal hypersensitivity via GPR40, iScience 27 (2024) 110552, https://doi.org/10.1016/j.isci.2024.110552.
[103] A. Czauderna, G. Kulkarni, N. Bianchi, L. Cheng, M. Sim, N.R. Realini, J. Gach, A. Caillon, J. Kloehn, G. Lambeau, A. Hausmann, S. Serra, M.T. Sorbara, S. Becattini, Long-chain unsaturated fatty acids released during immune responses stimulate host-microbe trans-kingdom communication, Cell Host Microbe 33 (2025) 1–19, https://doi.org/10.1016/j.chom.2025.08.011.
[104] Y. Sui, X. Hou, J. Zhang, X. Hong, H. Wang, Y. Xiao, X. Zeng, Lipid nanoparticle-mediated targeted mRNA delivery and its application in cancer therapy, J. Mater. Chem. B. (2025), https://doi.org/10.1039/d5tb01556a.
[105] D. Pozzi, G. Caracciolo, Looking back, moving forward: lipid nanoparticles as a promising frontier in gene delivery, ACS Pharmacol. Transl. Sci. 6 (2023) 1561–1573, https://doi.org/10.1021/acsptsci.3c00185.
[106] H. Li, Y. Wang, Q. Tang, D. Yin, C. Tang, E. He, L. Zou, Q. Peng, The protein corona and its effects on nanoparticle-based drug delivery systems, Acta Biomater. 129 (2021) 57–72, https://doi.org/10.1016/j.actbio.2021.05.019.
[107] J. Szebeni, P. Bedőcs, R. Urbanics, R. Bünger, L. Rosivall, M. Tóth, Y. Barenholz, Activation of complement by therapeutic liposomes and other lipid excipient-based therapeutic products: prediction and prevention, J. Control. Release 160 (2012) 382–387, https://doi.org/10.1016/j.jconrel.2012.02.029.